



Evaluation of physicochemical characteristics, bioactive properties, drying kinetics, and rehydration of convective dried autumn olive berries as a source of functional food ingredients

Awadalgeed M. A. Hassan^{1,2} · Ilkay Koca¹

Received: 19 March 2022 / Accepted: 5 August 2022 / Published online: 26 August 2022

© The Author(s), under exclusive licence to Springer Science+Business Media, LLC, part of Springer Nature 2022, corrected publication 2022

Abstract

Autumn olive berries (AOBs) are a good source of natural antioxidants and compounds associated with protective effects on health. The current study investigated the possible impacts of the convective drying process on textural, morphological, phenolic compounds, and antioxidant properties of AOBs. Four drying temperatures (50, 60, 70, and 80 °C) in addition to three air velocities (0.5, 1.0, and 1.5 m/s) were applied. The fresh AOBs contained 77.90% moisture, 4.37 pH, and 16.90% total soluble solids. The phytochemical data of the fresh sample revealed that it contained 1739.95 mg/kg total phenolic (TPC), 4370.69 mg/kg total flavonoid (TFC), 150.69 mg/kg lycopene content (LC), 50.20 mmol/g DPPH and 37.38 mmol/g FRAP. Furthermore, the TPC, TFC, lycopene, DPPH, and FRAP values of dehydrated AOBs were evaluated. It was observed that the convective drying increased the TPC, TFC, and antioxidant properties under all the drying conditions, giving the highest values at 80 °C. The AOBs dried at 80 °C contained the highest level of 96,592.22 mg/kg TPC, 476.97 mg/kg LC, 6.57 mg/kg gallic acid, 9.66 mg/kg catechin, 1.80 mg/kg benzoic acid, 2.13 mg/kg salicylic acid, 37.24 mg/kg ellagic acid, and 8.83 mg/kg quercetin-3-glucoside. Fruits dried at 60 °C contained 1873.09 mg/kg, a higher flavonoid content. The TPC, TFC, LC, and DPPH, increased with dried compared with fresh state. The color values (L^* , a^* , and b^*) of AOBs were decreased by drying, and the highest level of ΔE (10.89) was detected at 50 °C. Furthermore, the dried autumn olive at 80 °C and 1.5 m/s air velocity provided high hardness, chewiness, and gumminess of 6764.23, 1691.83, and 2989.16, respectively. The result of drying air velocities revealed no significant effects on rehydration, textural properties, and total color change. The air velocity of 1.5 m/s presented the highest values of shrinkage, hardness, antioxidant contents, and antioxidant activity for all dried samples than other air velocities. Midilli model was the best-fitted model describing the drying kinetic of AOBs, and the Weibull model described well the rehydration behavior of dried AOBs. The dried AOBs were statistically much more hardness, gumminess, and chewiness than the fresh AOBs. The present study highlighted the potential of dried AOBs as a good source of various nutrients that maintain human health with higher antioxidant properties compared with fresh fruit. These results indicate that the best drying conditions to have dried AOBs with high antioxidant properties were at 80 °C and 1.5 m/s. The dried AOBs obtained at these drying conditions can be used on the industrial scale for multi-purposes.

Keywords Autumn olive berries · *Elaeagnus umbellata* · Drying kinetics · Phenolics · Rehydration

Introduction

Autumn olive (*Elaeagnus umbellata*) is native to East Asia, and it is considered an invasive plant in some regions of the [1]. The Autumn olive plant produces small edible deep-red round berries with a sweet-tart taste, and it is consumed in Korea, China, and Japan [2]. In the USA annual production of 4-year-old plants is approximately 8.8 kg of autumn olive berries (AOBs) [3]. Many fruits contain health-promoting compounds including phenolic acids, anthocyanins, tannins, and flavonoids [4]. AOBs are an excellent source of vitamins

✉ Awadalgeed M. A. Hassan
awad114@yahoo.com

✉ Ilkay Koca
itosun@omu.edu.tr

¹ Department of Food Engineering, Faculty of Engineering, Ondokuz Mayıs University, 55139 Samsun, Turkey

² Department of Food Technology, Faculty of Agriculture, Red Sea University, Port Sudan, Sudan

and minerals, flavonoids, bioactive compounds, and essential fatty acids [5]. Proper consumption of natural antioxidant compounds plays a critical role in maintaining human health from the risk of chronic diseases, which is done by inhibiting or reducing oxidative stress [6, 7]. Carotenoids, e.g., lycopene, are essential natural fat-soluble pigments synthesized principally in plants. Red fruits and vegetables contain lycopene in varying amounts, and their processed products, such as juice, ketchup, paste, sauce, and soup, are also good dietary sources of lycopene [8]. AOBs have considerable antioxidant capacity since their high total phenolic compounds such as phenolic acids, flavonoids, tannins, and anthocyanins [9]. Recent evidence suggests that AOBs have a considerable antioxidant activity and high lycopene content of about 26 mg/100 g fresh weight [10]. In addition, AOBs contain vitamin C (13.8–16.9 mg/100 g), essential oils, and minerals such as Fe, Mg, P, Na, and K [11]. Additionally, AOBs contain a valuable source of polyphenols and α - and γ -tocopherols [2].

A growing body of literature recognizes the importance of AOBs. Studies of AOBs, such as that conducted by Ahmad et al. [5], have shown fruits, flowers, and seeds to treat several diseases like cough and cancer. In addition, AOBs are a rich source of carotenoids, phenolic acids, and flavonoids and are one of the widely used for the prevention of many diseases [12], reducing blood pressure, coughs, and pulmonary infections [13]. Furthermore, AOBs have a pivotal role in lowering blood glucose during fasting and postprandial due to a considerable impact on inhibiting the α -glucosidase enzyme [14]. Spinola et al. [15] reported that the leaves and berries of autumn olives as natural sources of biologically active compounds positively lower diabetes and obesity. Furthermore, this fruit contains 18 times more lycopene than tomato to be eaten fresh or processed as a flavoring or alternative to tomato products [16]. Recently researchers have become more interested in using AOBs to produce lycopene-rich extracts or powders for food formulation in commercial production [2].

Conservation techniques are applied to extend the shelf life of fruits and maintain their nutritional value. The fresh fruits are processed by drying to avoid perishability due to their high moisture content and the seasonal nature of their production. Furthermore, natural dried products can be transported cheaply for distribution to areas with a permanent shortage of fruits and vegetables [17]. Drying is a common and old method that prevents food microbial and chemical spoilage and enhances shelf life by decreasing water activity [18]. Dehydration is collectively used to include all drying methods in which water removal is carried out under controlled conditions of temperature, humidity, and airspeed. The use of hot air is the most common method of artificial drying process [19]. AOBs are seasonal fruits that naturally deteriorate due to their high water content and

other biological activities. The higher temperature of the air increases the evaporation rate of water from the product so that the rate of drying increases [20]. Putra and Ajiwignu [21] studied the effect of air temperature on the drying process and concluded that the effect of temperature is less significant at high air velocity. The convective drying of fruits is the most applied drying technique to stabilize fruits against physicochemical degradations and increase shelf life. The convective drying method occurs by exposure to heat when the stream of hot air flows over the food, leading to its dehydration [22]. Mathematical modeling is a valuable tool in drying, optimizing, and designing dryers. Zannou et al. [12] concluded that the optimum drying condition of AOBs at 81 °C and air velocity of 1 m/s, to preserve the phenolic compounds, lycopene, antioxidant capacity, and good color. The modeling contains complex partial differential equations to express heat and mass transfer, which can solve by different analytical and numerical methods [23]. The drying at high air velocities causes inner resistances to control the transport mechanisms inside the product, which causes significant shrinkage [24]. Majdi et al. [25] observed that the air temperature had a notable influence on drying time, energy consumption, and shrinkage, but the effect of air velocity was most important in shrinkage. The shrinkage of the structure depends on the drying method, air temperature, and air velocity [26]. The studies of kinetic are necessary to control the process of drying, and preservation of phytochemical compounds and the nutritional value of AOBs. The drying kinetics is often used to describe the mechanisms of heat and mass transfer during drying and it is fundamental to controlling the optimization of natural materials [27]. Previously, studies have been carried out on the drying and rehydration kinetics of *E. umbellate*, *Rosa pimpinellifolia*, lemon slices, and strawberry fruits [12, 28–30].

Most of the convective drying studies of AOBs have not been carried out at a different temperature and have not dealt in much detail with its drying and rehydration kinetics. The structural and physical characteristics of AOBs are changed during the drying due to water evaporation and increased solids. One of the most commonly used compression tests in food studies is tissue profile analysis (TPA). The sample is subjected to two consecutive compression events that mimic a jaw movement [31]. It is used to provide precise force, time, distance, and deformation [32], which can also calculate hardness, fragility, springiness, cohesion, stickiness, cohesiveness, and chewing values. Rehydration is an important feature used to understand the quality of dried fruits. It can be considered a measure of the physical and chemical changes during drying fruits. During the drying process, water migrates from the inner cells of the food through cell membranes and walls to diffuse within the porous structure towards the drying medium. These moisture gradients and microstructural stresses cause shrinkage and deformation of food products. Therefore, the

rehydration value is an important quality parameter in dried foods [33]. Rehydration capacity and rate concerning drying are the most evaluated quality characteristics in the literature [29, 34, 35]. Water absorption is a phenomenon that can be explained by physical or empirical models based on concepts of chemical kinetics. In this work, the rate of rehydration of dried products has been extensively discussed. The drying and rehydration kinetics modeling was investigated using empirical models to determine the best-fitted models. To date, no study has investigated the convective drying conditions to preserve the phytochemical compounds, antioxidants, shape, color, and texture of AOBs. Thus, this paper attempts to determine the impact of convective drying on the physical, textural, morphological, and bioactive properties of AOBs. It represents a significant opportunity to locally produce dried AOBs in the Turkish area by advancing our understanding of fruit drying characteristic. This study establishes optimum drying conditions and determines the drying and rehydration kinetics of autumn olive fruits.

Materials and methods

Preparation of plant material and sample extract

The whole mature autumn olive fruits were collected from the experimentation field of the Department of Horticulture, Ondokuz Mayıs University at Samsun, Turkey. The fruits Samples brought to the laboratory were washed, removed from excess water, and sorted in the refrigerator at +4 °C.

Chemicals and reagents

Methanol, ethyl acetate, hexane, hydrochloric acid, ethanol, acetic acid, sodium nitrite, sodium hydroxide, Folin–Ciocalteu reagent, 2,2-Diphenyl-1-Picrylhydrazyl (DPPH), 2,4,6-Tris (2-pyridyl)- 1,3,5 triazine (TPTZ), Trolox (6-hydroxy 2,5,7,8-tetramethylchroman-2-carboxylic acid), were purchased from Sigma-Aldrich. Aluminium chloride, Folin–Ciocalteu, Iron chloride and were purchased from Merck. Hexane from TEKKİM, and Butylated hydroxytoluene from SAFC. Gallic acid and Sodium carbonate were purchased from Riedel–de Haen. Potassium chloride, sodium acetate, and glacial acetic acid were purchased from Carlo Erba.

Physico-chemical characteristics and antioxidant properties of fresh fruits

Determination of total soluble solids

After the pulp fruits were homogenized with 10 g of crushed fruit with 20 mL of distilled water and filtered through filter paper, they were dropped into the Abbe refractometer

(Atago, Japan), and the total soluble solids were evaluated at room temperature of 20 °C [28].

Determination of fruit flesh to seed ratio (F/S)

The seeds to fresh fruits ratio (S/F) was determined by weighing the flesh and seeds separately. Then the ratio was calculated using Eq. (1).

$$S/F = \frac{S_w}{F_w} \quad (1)$$

where S_w is the weight (g) of the seeds and F_w is the weight (g) of the fruit flesh.

Water activity

Water activity was determined for both fresh and dried samples using Water Activity Meter (Aqualab Dewpoint,4TE, ABD).

PH analysis

It was carried out with a pH meter, and the sample was diluted with distilled water at 1:10 [36].

Titration acidity

A certain amount of the sample was prepared for pH analysis using a pH meter (Model Starter 3100, OHAUS, Parsippany, NJ, USA), and a measuring cylinder. It was measured by titrating a mixture of autumn olive juice (10 mL) diluted in distilled water (100 mL) with 0.1 M NaOH solution until the pH reached eight. The concentration of acid was expressed as % of malic acid. The titration acidity was determined by the amount of alkali consumed.

Drying procedure

The drying system was a laboratory-scale cabinet dryer (EKSIS, Isparta, Turkey) functioning in the convective dryer achieved according to Pashazadeh et al. [28]. The drying experiments were done at constant temperatures of 50, 60, 70, and 80 °C, and air velocities of 0.5, 1.00, and 1.5 m/s. The endpoint of the drying process was when the weight of autumn olive fruits reached a constant level, and moisture content decreased from 1 g water/g dry matter to approximately 0.02 g water/g dry matter of about 2% or less (wet basis). The drying time varied from 22 h for the dryings at 50 °C, 0.5 m/s to about 2 h at 80 °C, 1.5 m/s. The moisture content of the samples was determined by weight loss during the drying.

Modeling of drying kinetics

Experimental values include the variation of the humidity values obtained during the drying process, modeled with the drying time. The moisture ratio (MR) was determined with Eq. (2):

$$MR = \frac{M_t}{M_0} \quad (2)$$

where M_0 and M_t are initial moisture and at time t , respectively.

The drying kinetics of autumn olive fruits were fitted to 9 models listed in Table 1. The coefficient of determination (R^2), chi-square (X^2), and root mean square error (RMSE) were calculated to find the best model to predict the dehydration kinetics. This mathematical modeling also was determined by MATLAB software (R2016b) and calculated according to Pashazadeh et al. [28] with the following equations:

$$R^2 = 1 - \left(\frac{\sum_{i=1}^N (MR_{p,i} - MR_{e,i})^2}{\sum_{i=1}^N (MR_{e,i} - MR_{e,i})^2} \right) \quad (3)$$

$$X^2 = 1 - \left(\frac{\sum_{i=1}^N (MR_{e,i} - MR_{p,i})^2}{N - n} \right) \quad (4)$$

$$RMSE = \left(\frac{1}{N} \sum_{i=1}^N (MR_{e,i} - MR_{p,i})^2 \right)^{1/2} \quad (5)$$

The experimental ($MR_{e,i}$) and the predicted moisture rates ($MR_{p,i}$). The mean of the experimental moisture ratio is ($MR_{e,i}$). N is the number of treatments, and n is the number of constants in the models.

Rehydration capacity

The dried samples were rehydrated by dipping approximately 5 g in 500 mL of distilled water at room temperature (25 °C) for 12 h, performed according to Pashazadeh et al. [28].

The moisture content during the rehydration process was calculated on a dry basis (d.b), as shown in Eq. (6):

$$Mc = \frac{W_{st} - W_{dm}}{W_{dm}} \quad (6)$$

where Mc is the moisture content at any time (d.b), W_{st} is the weight of the sample (g) at any time, and W_{dm} is the dry weight (g) for their treatment.

The rehydration ratio (R_r) of dried AOBs was determined using the following equation:

$$R_r = \frac{M_t - M_0}{M_e - M_0} \quad (7)$$

where M_t , M_0 , and M_e are the water contents at time t , before rehydration, and end of rehydration, respectively.

The rehydration kinetics modeling for dried fruits was performed by comparing six models, including Peleg, first-order kinetic, Exponential related, Exponential, Weibull, and Vega-Gálvez models (Table 2). These models have been successfully applied in several studies to be the well fit models for the rehydration kinetics [28, 37, 38]. Model with the highest R^2 , lowest X^2 and lowest RMSE were selected as the best model to predict the dehydration kinetics. The data on rehydration kinetics of autumn olive fruits were statistically compared according to the values of coefficient of determination (R^2), chi-square (X^2), and RMSE using MATLAB software (R2016b). The applied models explain the rehydration behaviors of dried fruits.

Table 1 Models applied to the drying curves of *E. umbellata*

Models	Equations	References
Newton	$MR = \exp(-kt)$	[80]
Page	$MR = \exp(-ktn)$	[52, 81]
Henderson and Pabis	$MR = \alpha \exp(-ktn)$	[52, 81]
Logarithmic	$MR = \alpha \exp(-ktn) + c$	[53, 81]
Two term	$MR = \alpha \exp(-kt) + b \exp(-gt)$	[53]
Wang and Singh	$MR = 1 + at + bt^2$	[53]
Approximation of diffusion	$MR = \alpha \exp(-kt) + (1 - \alpha) \exp(-kbt)$	[82]
Logistic	$MR = \alpha / (1 + b \exp[kt])$	[83]
Midilli	$MR = \alpha \exp(-ktn) + bt$	[52, 53]

MR is the moisture ratio; t is the time; and α , b , c , g , and k are the constants of models

Table 2 Models applied to the rehydration kinetics of *E. umbellata*

Model	Equations	References
Peleg	$Rr = 1 + \frac{1}{Xe-X0} + \frac{t}{\alpha+bt}$	[71]
First-order kinetic	$Rr = 1 - \exp(-\alpha t)$	[38, 57]
Exponential related	$Rr = 1 - \exp(-\alpha t)$	[38, 84]
Exponential	$Rr = 1 - \exp(\alpha t^k)$	[57, 85]
Weibull	$Rr = 1 - \exp\left(-\left(\frac{t}{b}\right)^\alpha\right)$	[57, 71]
Vega-Gálvez	$Rr = \alpha \exp \times \frac{-b}{(1+t)^k}$	[38, 71]

Where Rr is the rehydration ratio; t is the time; and α , b, and k are the constants of models

Texture measurements

Fruit texture was measured using one of the most commonly used compression tests, Texture Profile Analysis (TPA), with a texture analyzer (model TA.XT.Plus, Stable Micro Systems, Godaming, Surrey, UK). The sample was subjected to two consecutive compression events, imitating a jaw s movement. The compression samples was applied by applying TA-24 1/4 dia. cyl., acrylic, 35 mm tall cylinder probes, and a compression plate of a 50 kg load cell. Thus, a force–deformation curve can be obtained from (TPA). In addition, one can calculate hardness, fracturability, springiness, cohesiveness, adhesiveness, gumminess, and chewiness values observed in different drying temperatures [31, 39].

Scanning electron microscope (SEM)

Scanning electron microscopy SEM (JEOL JSM-7001F) was used to obtain the microstructures of the fresh and dried AOBs with high resolution, at the research center of KITAM, Samsun, Turkey. First, fresh and dried samples were taken from autumn olive berries as a small specimen with a special knife to examine plant surfaces and attached to a stainless stub. Then the samples were immediately coated with gold/palladium (60/40) at approximately 10 nm, functioning with argon and plasma current for 2 min. The SEM images were recorded at 200 \times magnification and an acceleration voltage of (10.0 kV).

Surface area and shrinkage of fruits

An image acquisition system consisting of a color camera for capturing an overhead view of the samples, a frame grabber to capture the vie followed by a lighting room, then the images were treated by computer software. Calibration was first made with precision drawings of 15 AutoCAD 2021 (Autodesk Inc., San Rafael, CA). Lastly, the fruit area was obtained by converting the number of pixels to actual

dimensions. Then, image analysis measurements were tested with Auto CAD 2021 precision drawings.

Total color change

The color parameters of fresh samples and after drying, L* [brightness. 100 = white; 0 = dark), + a* (+ red; – green), + b* (+ yellow; – blue), were determined using a colorimeter (Model DP 400, Minolta, Japan)], according to Pashazadeh et al. [28].

The total color change (ΔE) between fresh and dried autumn olive fruits was determined with Eq. (8):

$$\Delta E = \sqrt{(\Delta L^*)^2 + (\Delta a^*)^2 + (\Delta b^*)^2} \quad (8)$$

where ΔL^* , Δa^* , and Δb^* are the differences between L*, a*, and b* before and after drying, respectively.

Antioxidant activity and bioactive compounds

The extractions were carried out by weighing 2 g of dried sample and 5 g of fresh sample, mixed with 20 mL of 80% methanol, and left for 12 h at 25 °C. The mixtures were filtered and properly diluted for the analyses.

Total phenolic content (TPC)

The Total Phenolic of Autumn olive extracts was determined using the Folin-Ciocalteu modification method according to Zannou and Koca [40]. First, Folin-Ciocalteu reagent was added to the appropriately diluted samples. Then, after waiting for 5 min in the dark, saturated sodium carbonate (Na_2CO_3) solution was added to the mixture. Finally, it was mixed and left in the dark for 2 h and read at 760 nm using (Agilent Technologies Spectrophotometer, Cary 60, Australia).

Total flavonoid content (TFC)

The total flavonoid was measured by a modified protocol test according to Fawole et al. [41]. First, sodium nitrite solution (5%, 0.15 mL) was added to the sample and reacted for 5 min, followed by 0.3 mL of 10% aluminium chloride. After 5 min, 1 mL of 1 M sodium hydroxide was added. Finally, the spectrophotometer absorbance of the mixture was measured at 510 nm.

Lycopene content

Lycopene content from AOBs was measured according to the method detailed by Ghellam and Koca [10] which used a mixture (2:1:1) of hexane, methanol, and acetone (containing 0.05% BHT) was added to a determined weight of

autumn olives pulp, kept under 200 rpm at room temperature ($\approx 20\text{ }^\circ\text{C}$) in an orbital shaken (ST 30, NÜVE. Turkey) for 30 min. After that, 3 mL of distilled water was added to the mixture, and then it was shaken for 3 min. The pulp was extracted many times till being colorless. To separate the red non-polar from polar solvents, the mixture was left for 10 min for decantation. The lycopene content (mg/100 g FW) was calculated following Eq. (9):

$$\text{Lycopene (mg/100mg FW)} = \frac{A_{502}}{17.2 \times 10^4 \text{ L/mole/cm}} \times \frac{1}{b \text{ cm}} \times \frac{536.9 \text{ g}}{\text{mole}} \times \frac{11}{10^3 \text{ mL}} \times \frac{10^3 \text{ mL}}{100 \text{ g}} \times \frac{V \text{ mL}}{\text{kg tissue}} \times \frac{\text{kg}}{10^3 \text{ g}} \quad (9)$$

where A_{502} is the absorbance at 502 nm, b is the light path, and V is the volume of non-polar solvent.

DPPH free radical scavenging activity

50 μL of methanol extracted samples were taken and mixed with 1 mL of DPPH solution, and their absorbance was determined at 517 nm wavelength after 2 h [42]. The DPPH solution was used as a control, and the scavenging ratio was calculated with Eq. 3. The DPPH radical scavenging-based antioxidant activity was assessed from a calibration curve and expressed as Trolox equivalent (mmol TE/g).

$$\text{Reduction(\%)} = \left(\frac{A_c - A_s}{A_c} \right) \times 100 \quad (10)$$

Ferric reducing antioxidant power (FRAP)

The ferric reducing ability (FRAP) of AOBs methanolic extracts was diluted at the appropriate rate; mixed with a mixture of 300 mM acetate buffer: 20 mM FeCl_3 : 10 mM TPTZ solution (dissolved in 40 mM HCl) at a ratio of 10:1:1 (v:v:v) to determine the absorbance at 593 nm in a spectrophotometer (Thermo Spectronic, UK). With the help of solutions prepared with FeSO_4 , a calibration curve was drawn, and antioxidant capacity was calculated [43].

Liquid chromatography-tandem mass spectrometry (LC-MS/MS) analysis

The phenolic compounds of fresh and dried samples were determined using liquid chromatography coupled to a mass spectrometer detector (LC-MS/MS, Shimadzu LC-MS 8040) via electrospray ionization (ESI) and two pumps (LC-30 AD), a column oven (CTO-10AS VP), an autosampler (SIL-30AC) and a degassing unit (DGU-20A 3R) [12]. The phenolic compounds were identified based on their elution time and quantified from their peak area. The identified compounds were quantified using a mixture of external standards

gallic acid, catechin, fumaric acid, and quercetin) prepared by dissolving standards in methanol at concentrations of 0, 50, 75, 100, 150, and 200 ppm.

Statistical analysis

Statistical analysis was performed using SPSS Statistics software v.26 (IBM SPSS Statistics for Windows, IBM Corp., USA). Data of all analysis, in triplicate, are expressed as mean \pm standard deviation. In addition, the significant differences between the samples were determined by performing the analysis of variance (ANOVA) in a Tukey's test (at $p < 0.05$). The MATLAB software (R2016b) was used for the modeling.

Results and discussion

Physico-chemical and antioxidant properties of fresh AOBs

Prior studies noted that the AOBs have considerable antioxidant activity and lycopene content [10, 16], and health-promoting compounds, such as phenolic compounds and flavonoids and flavonoids [4, 9]. As shown in Table 3, AOBs are almost spherical fruits (7.29 mm in width and 7.34 mm in length) with a seed/Flesh ratio of 8.5 and a mean weight of 0.26 g for each berry at the fully ripe stage. These findings are slightly higher than those conducted by Wu et al. [44] and Gamba et al. [9]. The dry matter, pH, total soluble solids, and water activity were 22.11%, 4.37, 16.90%, and 0.96, respectively. Many studies, to some extent, go in line with these findings [9, 10, 12]. According to Gamba et al. [9], the *E. umbellata* is a good source of health-promoting bioactive compounds. Ghellam and Koca [10] reported that the AOBs have 1052.48, 30.56, 26.66, and 8.58 mg/100 g total phenolic compounds (TPC) flavonoid content (TFC) and vitamin C, respectively. L^* , a^* , and b^* values were 42.50, 13.09, and 11.06, respectively. Previous research reported similar results [12], except for the a^* value, which turned out to be slightly higher. As mentioned in Table 3, another important finding is that the total phenolic content was 1739.95 mg/kg; this result is close to that of Wang and Fordham [45], which observed total phenols found in AOBs ranging from 190 to 275 mg/100 g fresh weight. The total flavonoid content was 437.69 mg/kg, and this finding is slightly inconsistent with Khattak [46], which observed that the total flavonoid of AOBs is 103 mg/100 g. As shown in Table 3, the lycopene content of fresh autumn olive berry fruits yielded 150.70 mg per kg; this result differs from Ghellam and Koca [10] estimate of lycopene content (26 mg/100 g fresh weight), but they are broadly consistent with Fordham et al. [16], that

Table 3 Physico-chemical and antioxidant characteristics of fresh AOBs

Parameter and unit	Mean value \pm SD
Width, mm	7.29 \pm 0.50
Length, mm	7.34 \pm 0.35
Fruit weight, g	0.26 \pm 0.02
Seeds weight, g	0.02 \pm 0.002
Seed/flesh ratio, %	8.5 \pm 1.06
TSS, Brix	16.90 \pm 1.77
Moisture, %	77.9 \pm 4.21
pH	4.37 \pm 0.28
Water activity	0.96 \pm 0.004
Titrateable acidity (malic acid), %	2.83 \pm 1.0456
Total phenolic compound, mg/kg	1739.95 \pm 213.93
Flavonoid, mg/kg	437.69 \pm 28.86
FRAP, mmol/g	37.38 \pm 5.21
DPPH, mmol/g	50.20 \pm 6.78
Lycopene, mg/kg	150.70 \pm 13.72
Color	
L*	42.50 \pm 1.41
a*	13.09 \pm 1.55
b*	11.06 \pm 0.57

Means values of three replicates and corresponding standard deviations

found lycopene content ranged from 15 to 54 mg/100 g in fresh fruits. The values of DPPH and FRAP were 50.20 and 37.384 mmol/g, respectively. Ishaq et al. [47] reported that many extracts of autumn olive TPC and TFC ranged from 16.3–20.0 mg/g and 1.5–3.8 mg/g, respectively (see Fig. 1).

Modeling of drying kinetics

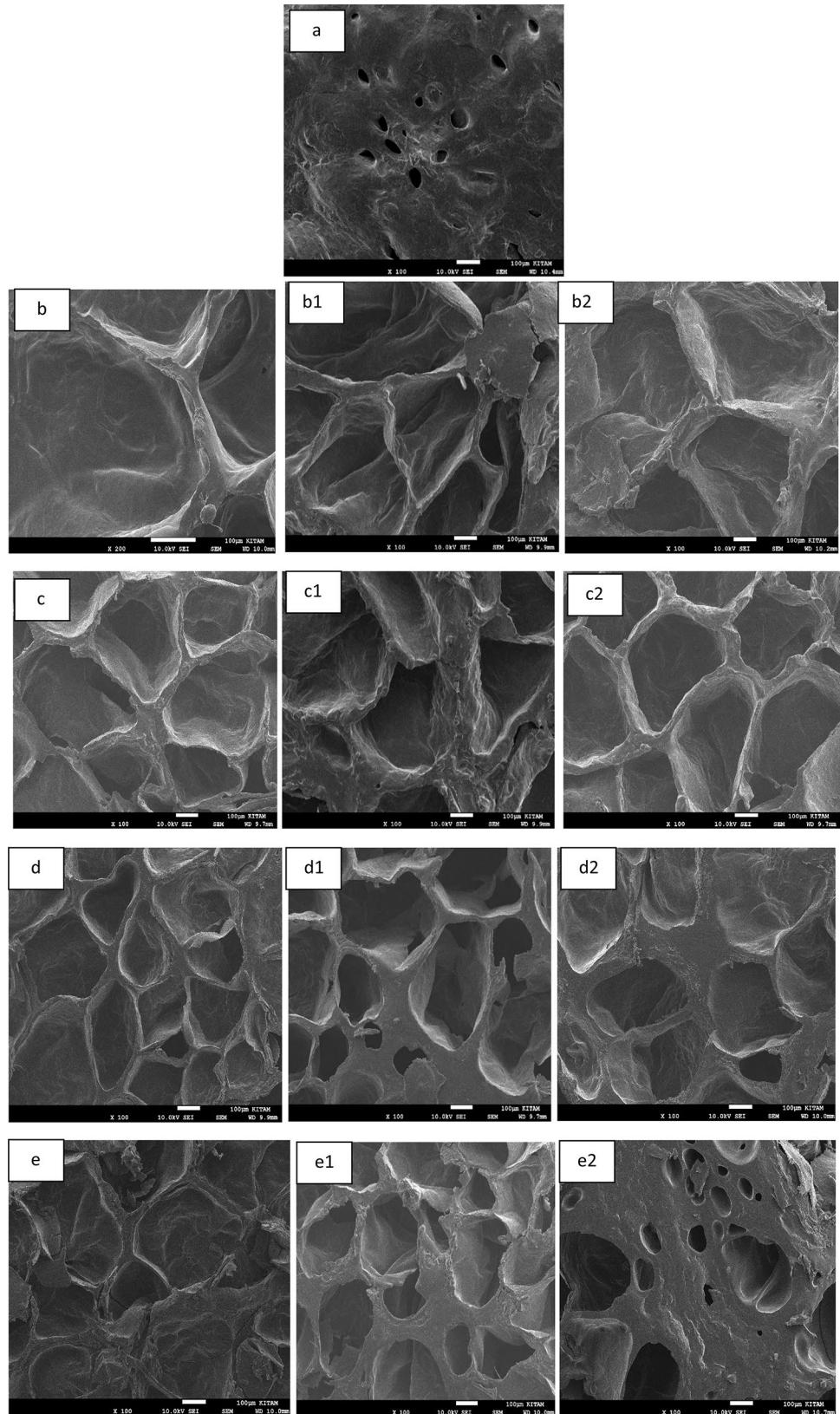
The fresh AOBs were submitted to the convective drying considering the combination of four temperatures (50, 60, 70, and 80 °C) and three air velocities (0.5, 1, and 1.5 m/s). The drying data of AOBs was applied to nine empirical drying models and the results were shown separately in Table 1. The moisture content of AOBs decreased continuously with drying time. Figures 2, 3, and 4 shows the drying curves obtained for AOBs as a function of temperature, air velocity, and relative moisture of the drying air. As shown in Fig. 2, the time to reach the constant moisture contents differed for the same air velocity of 0.5 m/s and different temperatures, being 1340 min at 50 °C, 840 min at 60 °C, 300 min at 70 °C, and 240 min at 80 °C. Similarly, as can be seen in Fig. 3, the time to reach the constant moisture contents at 1.0 m/s was 1230 min at 50 °C, 720 min at 60 °C, 210 min at 70 °C, and 150 min at 80 °C. In addition, for the air velocity of 1.5 m/s, the time to reach the constant moisture contents was 960 min at 50 °C, 360 min at 60 °C, 180 min at 70 °C,

and 120 min at 80 °C. Thus, the drying time decreases with the increase in drying temperature, supporting evidence from previous observations [48, 49]. Izli et al. [50] found that the drying time was reduced by combining microwaves with conventional drying. The drying kinetics were applied to Newton, Page, Hendeon, and Pabis, Two-term, Two-term exponential, Logistic, and Midilli models due to a well-fitted description of the dehydration behavior. Applying models in the present study shows similarities to those described by Zannou et al. [12] and Pashazadeh et al. [28]. Mathematical modeling was also calculated according to high R^2 , low RMSE, and X^2 values were determined in Table 4. The drying curve was applied to the Midilli model due to a well-fitted description of the dehydration behavior (Fig. 5). Pashazadeh et al. [51] reported that the Midilli model best describes the drying kinetic of the *rosa pimpinellifolia* fruits. The Midilli model [52, 53] describes the drying characteristics of AOBs and the heat and mass transfer phenomena during the drying process. The higher coefficient of determination (R^2) and the lower chi-square (X^2), the better the fitness of the mathematical model to the experimental data. In our study, the Midilli model at 80 °C and 1.5 m/s showed the highest values of $R^2 = 0.9998$, $RMSE = 0.006$ and $X^2 = 0.00005$, respectively. The current study showed Midilli model was observed to be more satisfactory for all the experimental data of AOBs with a higher value for R^2 and X^2 (Table 4), compared with the statistical values obtained for other models. These findings are consistent with Pashazadeh et al. [51], who also found that the Midilli model was the best-fitted model describing the drying kinetic of the *Rosa pimpinellifolia* fruits.

Rehydration kinetics and modeling

The rehydration experiments of autumn olive fruits dried at 50, 60, 70, and 80 °C and 0.5, 1.0, and 1.5 m/s air velocity were carried out for three different drying conditions. The rehydration curves for the different drying temperatures are shown in Fig. 6. The highest moisture content value of rehydrated fruit was 99.62% at 70 °C and 1.0 m/s air velocity. The lowest moisture content value was 96.13% at 50 °C 1.5 m/s air velocity. It is believed that the drying temperature affects the behavior of the fruits rehydrated at different temperatures, so the water permeability and water uptake rate in the rehydration capacity are associated with the increase in drying temperature, which could be attributed to some substances being carried by water flow during drying [54]. The current study found that the water uptake during rehydration was faster at first. Then the rate gradually decreased as the moisture content approached equilibrium. These results reflect those of García-Pascual et al. [55], who also found that the decrease in water intake of the samples after rapid absorption has been associated with the decrease in mass

Fig. 1 Morphology of AOBs tissue using scanning electron microscopy graphs ($\times 100$); **a** for fresh fruits; **b, b1, b2, c, c1, c2, d, d1, d2, e, e1, and e2** for convective-dried fruits at 50 °C: 0.5 m/s, 50 °C: 1.0 m/s, 50 °C: 1.5 m/s, 60 °C: 0.5 m/s, 60 °C: 1.0 m/s, 60 °C: 1.5 m/s, 70 °C: 0.5 m/s, 70 °C: 1.0 m/s, 70 °C: 1.5 m/s, 80 °C: 0.5 m/s, 80 °C: 1.0 m/s, and 80 °C: 1.5 m/s, respectively at the different drying conditions



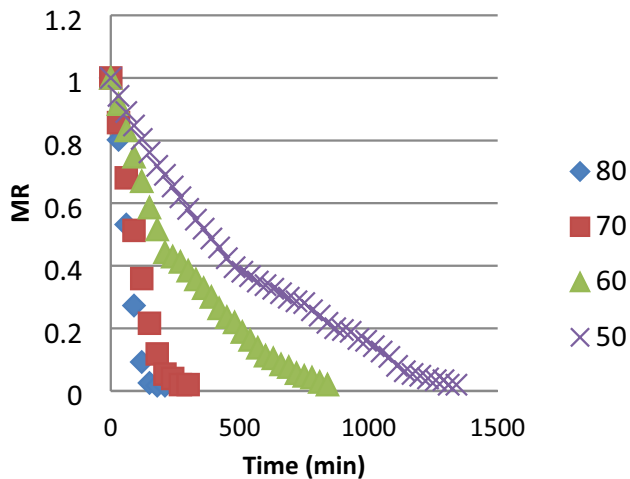


Fig. 2 Time-dependent moisture content changes of samples dried at 0.5 m/s air velocity at four different temperatures

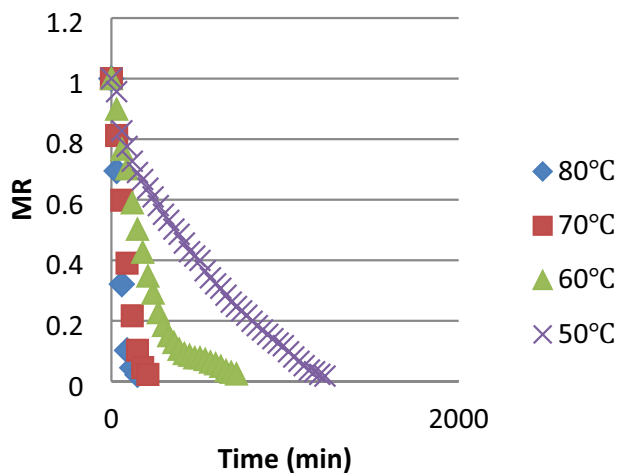


Fig. 3 Time-dependent moisture content changes of samples at 1.0 m/s air velocity at four different temperatures

transfer and the closeness of equilibrium. Another important finding was that the rehydration capacity was faster at 70 °C, followed by 80 °C, 60 °C, and 50 °C, respectively. The result also showed a different observation between the drying temperatures of the dried fruits. Prior studies that have noted the rehydration rate could be influenced by the drying temperatures, texture, and shape of the dried fruits [56]. The results of applied models explain that the rehydration kinetics of dried AOBs were recorded in Table 5. The changes in the time-dependent rehydration behaviors of AOBs dried at four different drying temperatures (50, 60, 70, and 80 °C) and air velocity of 1.0 m/s were showed separately for each temperature (Fig. 6). The rehydration kinetic models, including the Weibull model were applied to elucidate the mechanism controlling the rate uptake of water in dried AOBs during the

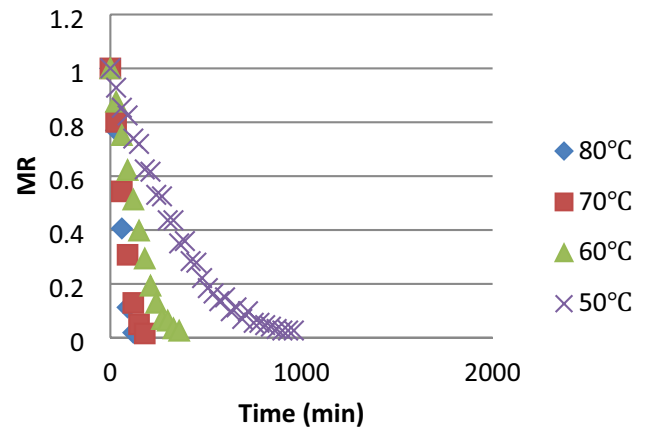


Fig. 4 Time-dependent moisture content changes of samples dried at 1.5 m/s air velocity at four different temperatures

rehydration process. The models with higher R^2 , as well as the lowest X^2 and RMSE, were selected as the best models to interpret the rehydration behaviors of dried AOBs. The results of rehydration data applied to empirical models stood given in Table 5. The studied models represented better the rehydration kinetics of AOBs. Among these models, the Weibull model was frequently utilized and later improved for describing the rehydration of dried foods [57]. The Weibull model was selected to interpret the rehydration behaviors of dried AOBs since it presented the highest R^2 , lowest X^2 , and RMSE (Table 5). The fruits dried at 70 °C and 1.0 m/s showed the Weibull model fit the experimental data well and presented the highest $R^2=0.998$, the lowest RMSE=0.0126, and the lowest $X^2=0.000161$. The results of this study indicate that the dried AOBs rehydration time and moisture content decreased as the drying temperature increased (Fig. 6). As mentioned in Table 5, the Weibull model showed the highest R^2 , and lowest X^2 values, it was selected as the best model for AOBs rehydration. This finding supports evidence from previous observations [58]. The water filled almost all the pores of dried fruits, and the fruit regained a significant percentage of its original moisture content.

Textural properties of autumn olive fruits

A considerable amount of literature has been published on the texture properties of dried samples. These studies are found that the texture properties of dried samples dependent on the water interactions with cellular matrix behavior and soluble solid phase inside the tissue [59, 60]. The textural parameters analyzed (hardness (HAR), springiness (SPR), cohesiveness (COH), Gumminess (GUM), chewiness (CHE), and Resilience (RES) for the fresh and dried autumn olive fruits are presented in Tables 6. Moreover, the effects of convective drying conditions on the textural properties

Table 4 Mathematical models for drying kinetics

Model	Drying temperature (°C)	Air velocity, m/s	R ²	RMSE	X ²	Constants	
Newton	50	0.5	0.989059	0.028375	0.000805	k=0.02827	
		1.0	0.983328	0.03397	0.001154	k=0.030524	
		1.5	0.981413	0.040085	0.001607	k=0.044429	
	60	0.5	0.992522	0.023602	0.000557	k=0.051069	
		1.0	0.991259	0.026443	0.000699	k=0.075886	
		1.5	0.958234	0.066482	0.000731	k=0.1022	
	70	0.5	0.951449	0.075019	0.005628	k=0.13811	
		1.0	0.953876	0.073882	0.005459	k=0.17255	
		1.5	0.941535	0.086173	0.007426	k=0.19562	
	80	0.5	0.942891	0.085449	0.007302	k=0.21032	
		1.0	0.952819	0.078957	0.006234	k=0.28395	
		1.5	0.909918	0.116625	0.013601	k=0.25315	
	Page	50	0.5	0.99119	0.025604	0.000656	k=0.021228 n=1.0775
			1.0	0.983456	0.034045	0.001159	k=0.02856 n=1.0183
			1.5	0.995306	0.020304	0.000412	k=0.020578 n=1.2353
60		0.5	0.99278	0.023401	0.000548	k=0.047017 n=1.0263	
		1.0	0.996265	0.017463	0.000305	k=0.051113 n=1.1437	
		1.5	0.995714	0.021736	0.000435	k=0.033677 n=1.4599	
70		0.5	0.998409	0.013933	0.000194	k=0.041063 n=1.5725	
		1.0	0.998293	0.014713	0.000216	k=0.061511 n=1.5459	
		1.5	0.999066	0.011377	0.000129	k=0.063191 n=1.6527	
80		0.5	0.998356	0.015007	0.000225	k=0.059697 n=1.7358	
		1.0	0.998991	0.012108	0.000147	k=0.11386 n=1.6593	
		1.5	0.999162	0.011928	0.000142	k=0.06085 n=1.977	
Hendeon and Pabis		50	0.5	0.989428	0.028048	0.000787	a=1.0165 k=0.02876
			1.0	0.983787	0.033703	0.001136	a=0.98243 k=0.029955
			1.5	0.986595	0.034312	0.001177	a=1.0689 k=0.047438
	60	0.5	0.992646	0.023617	0.000558	a=1.0099 k=0.051595	

Table 4 (continued)

Model	Drying temperature (°C)	Air velocity, m/s	R ²	RMSE	X ²	Constants
Logaritmik	70	1.0	0.993711	0.022661	0.000514	a=1.0504 k=0.079627
		1.5	0.97044	0.057083	0.000591	a=1.1047 k=0.11245
		0.5	0.966713	0.063731	0.004062	a=1.1221 k=0.15353
		1.0	0.96665	0.065028	0.004229	a=1.106 k=0.18953
		1.5	0.958045	0.076244	0.005813	a=1.1171 k=0.21713
		0.5	0.957921	0.075923	0.005764	a=1.1259 k=0.23297
	80	1.0	0.965063	0.07126	0.005078	a=1.1084 k=0.3104
		1.5	0.931586	0.1078	0.011621	a=1.1362 k=0.28402
		0.5	0.996223	0.016859	0.000284	a=1.1129 b=-0.13855 k=0.021146
		1.0	0.993992	0.020643	0.000426	a=1.127 b=-0.19441 k=0.019861
		1.5	0.994282	0.022589	0.00051	a=1.1381 b=-0.10891 k=0.0368
		0.5	0.994535	0.020546	0.000422	a=1.0403 b=-0.052043 k=0.045003
60	1.0	0.993807	0.022725	0.000516	a=1.0534 b=-0.006785 k=0.078021	
	1.5	0.992041	0.030258	0.000607	a=1.3068 b=-0.26023 k=0.069489	
	70	0.5	0.986079	0.042343	0.001793	a=1.2716 b=-0.19805 k=0.10399
		1.0	0.989658	0.03758	0.001412	a=1.3159 b=-0.26038

Table 4 (continued)

Model	Drying temperature (°C)	Air velocity, m/s	R ²	RMSE	X ²	Constants
						k=0.11797
		1.5	0.988511	0.041846	0.001751	a=1.4601
						b=-0.39846
						k=0.11629
	80	0.5	0.975336	0.06032	0.003639	a=1.2343
						b=-0.14446
						k=0.17194
		1.0	0.977269	0.060589	0.003671	a=1.2009
						b=-0.1191
						k=0.24045
		1.5	0.976338	0.067775	0.004593	a=1.6715
						b=-0.5914
						k=0.1281
Two-term	50	0.5	0.989038	0.02856	0.000816	a=0.0004500
						k=2.7679
		1.0	0.983959	0.033523	0.001124	a=0.026464
						k=1.121
		1.5	0.995062	0.020826	0.000434	a=1.7722
						k=0.061242
	60	0.5	0.992506	0.023841	0.000568	a=0.0006212
						k=2.1594
		1.0	0.991237	0.02675	0.000716	a=0.0002219
						k=1.7834
		1.5	0.992052	0.029599	0.000536	a=1.9534
						k=0.15502
	70	0.5	0.994273	0.026435	0.000699	a=2.0428
						k=0.21764
		1.0	0.993947	0.027703	0.000767	a=2.0193
						k=0.26974
		1.5	0.993654	0.029653	0.000879	a=2.0908
						k=0.31874
	80	0.5	0.992008	0.033088	0.001095	a=2.1234
						k=0.34005
		1.0	0.952773	0.082851	0.006864	a=0.0002036
						k=0.394167
		1.5	0.988895	0.043431	0.001886	a=2.2475
						k=0.4402

Table 4 (continued)

Model	Drying temperature (°C)	Air velocity, m/s	R ²	RMSE	X ²	Constants
Wang and Singh	50	0.5	0.98564	0.032689	0.001069	a=0.026089 b=0.0001215
		1.0	0.975895	0.041095	0.001689	a=0.029231 b=0.0001415
		1.5	0.996605	0.017268	0.000298	a=0.030212 b=0.0002858
	60	0.5	0.978128	0.040729	0.001659	a=0.048733 b=0.0003856
		1.0	0.98118	0.039202	0.001537	a=0.032346 b=0.0007250
		1.5	0.995072	0.023308	0.003524	a=0.058521 b=0.0013718
	70	0.5	0.990532	0.033988	0.001155	a=0.069422 b=0.0025561
		1.0	0.992935	0.029931	0.000896	a=0.046253 b=0.0038793
		1.5	0.98836	0.04016	0.001613	a=0.283224 b=0.0044955
	80	0.5	0.984792	0.045644	0.002083	a=- 0.15314 b=0.0058224
		1.0	0.985013	0.046672	0.002178	a=- 0.20812 b=0.01087
		1.5	0.972403	0.068467	0.004688	a=- 0.17311 b=0.0062228
Approximatin of diffusion	50	0.5	0.992299	0.024075	0.00058	a= 1.113 b=- 3.0928 k=0.021139 t= 3.1385
		1.0	0.988852	0.028294	0.000801	a= 1.0967 b=0.72868 k=0.025231 t=- 0.02639
		1.5	0.993503	0.024275	0.000589	a= 1.1346 b=0.065763 k=0.03416 t=0.93471
	60	0.5	0.994399	0.020996	0.000441	a= 1.0439 b=0.11463 k=0.046359

Table 4 (continued)

Model	Drying temperature (°C)	Air velocity, m/s	R ²	RMSE	X ²	Constants
						t=0.30016
		1.0	0.991973	0.026152	0.000684	a=1.0182 b=-0.018363 k=0.072531
		1.5	0.991576	0.031829	0.000746	t=0.59484 a=1.328 b=1.1228 k=0.064275
	70	0.5	0.986079	0.04357	0.001898	t=1.1135 a=1.2715 b=1.6891 k=0.10403
		1.0	0.989658	0.039115	0.00153	t=1.8007 a=1.3156 b=1.2811 k=0.1181
		1.5	0.988511	0.04411	0.001946	t=1.286 a=1.4604 b=1.0949 k=0.11621
	80	0.5	0.975335	0.062784	0.003942	t=1.1267 a=1.2338 b=1.6166 k=0.17182
		1.0	0.977269	0.064264	0.00413	t=1.7296 a=1.2009 b=1.4168 k=0.24046
		1.5	0.976338	0.073205	0.005359	t=1.5353 a=1.6705 b=1.0002 k=0.12818
Logistic	50	0.5	0.992299	0.024075	0.00058	t=0.98952 a=1.6091 b=2.5356 k=0.035778
		1.0	0.98791	0.029283	0.000857	a=1.1743 b=2.0171 k=0.039381

Table 4 (continued)

Model	Drying temperature (°C)	Air velocity, m/s	R ²	RMSE	X ²	Constants
		1.5	0.996479	0.017727	0.000314	a=0.63953 b=1.6105 k=0.070654
	60	0.5	0.992824	0.023545	0.000654	a=7.9036 b=8.8911 k=0.054527
		1.0	0.996327	0.017502	0.000306	a=1.5328 b=2.5505 k=0.10002
		1.5	0.997543	0.016813	0.000432	a=0.26069 b=1.2365 k=0.21276
	70	0.5	0.999173	0.010318	0.000106	a=0.20649 b=1.1993 k=0.3112
		1.0	0.999384	0.009174	0.0000842	a=0.21666 b=1.2048 k=0.38293
		1.5	0.999408	0.009502	0.0000902	a=0.17447 b=1.1747 k=0.47262
	80	0.5	0.999119	0.011399	0.00013	a=0.13308 b=1.1257 k=0.53599
		1.0	0.998696	0.014512	0.000211	a=0.18737 b=1.2052 k=0.67204
		1.5	0.998745	0.015607	0.000244	a=0.08502 b=1.0915 k=0.76088
Midilli	50	0.5	0.997568	0.013605	0.000185	a=1.0174 b=-0.001781 k=0.040308 n=0.84085
		1.0	0.998109	0.011654	0.000136	a=1.0268 b=-0.003366 k=0.071305 n=0.65715

Table 4 (continued)

Model	Drying temperature (°C)	Air velocity, m/s	R ²	RMSE	X ²	Constants
		1.5	0.996115	0.018773	0.000352	a=0.97488 b=- 0.000258 k=0.018418 n=1.2518
	60	0.5	0.996141	0.017427	0.000304	a=1.0312 b=- 0.001637 k=0.072027 n=0.85509
		1.0	0.998248	0.012219	0.000149	a=0.97662 b=0.000735 k=0.036829 n=1.2756
		1.5	0.997244	0.018205	0.000215	a=0.97513 b=- 0.001238 k=0.031229 n=1.4557
	70	0.5	0.998755	0.013029	0.00017	a=0.97867 b=2.628605 k=0.035249 n=1.6334
		1.0	0.998278	0.015959	0.0002ss55	a=1.0221 b=- 0.11463 k=0.000826 n=2.3946
		1.5	0.999445	0.009697	0.000090	a=0.993 b=- 0.00164 k=0.063282 n=1.6254
	80	0.5	0.998704	0.014393	0.000207	a=0.9795 b=0.000471 k=0.05103 n=1.8208
		1.0	0.999776	0.006384	0.000047	a=1.0033 b=0.0019306

Table 4 (continued)

Model	Drying temperature (°C)	Air velocity, m/s	R ²	RMSE	X ²	Constants
						k=0.11072
						n=1.7083
		1.5	0.999895	0.006074	0.000046	a=1.0033
						b=0.0019307
						k=0.11071
						n=1.7083

of autumn olive fruits were determined. The HAR, SPR, COH, GUM, CHE, and RES of fresh AOBs were determined at 206.39, 0.813, 0.673, 138.11, 112.48, and 0.326, respectively. The HAR, GUM, and CHE of samples processed by drying were several times higher than fresh fruits. While the fresh AOBs showed the highest values of SPR, COH, and RES (Table 6). Zielinska et al. [61] have shown that the cranberries processed by microwave vacuum drying were characterized by significantly greater hardness, gumminess, and chewiness than hot air convective drying samples. As seen in Table 6, the hardness, chewiness, and gumminess of dried fruits significantly increased with increasing temperature. Cruz et al. observed a decrease in hardness, chewiness, and cohesiveness for the drying of dried apples [62]. On the other hand, the springiness and cohesiveness values decreased when the drying temperature increased. The reduction in springiness and cohesiveness may be attributed to a loss of cell structural integrity during drying due to moisture loss. The dried autumn olive at 80 °C and 1.5 m/s air velocity provided high values with the hardness, chewiness, and gumminess of 6764.23, 1691.83, and 2989.16, respectively (Table 6). In this study, all the textural parameter values of dried samples had no clear relationships with drying air velocities, except the hardness values affected by air velocities of 0.5 m/s, 1.0, and 1.5 m/s were 2586.21, 2450.35, and 3197.12, respectively. Our findings showed that the drying conditions affected the textural properties of the AOBs. The HAR, GUM, and CHE values were increased, and SPR, COH, and RES values were decreased with the increase in drying temperature. The drying air velocities showed no textural differences between the SPR, COH, GUM, CHE, and RES of the AOBs, but the hardness values were affected by air velocities (Table 6).

Impact of different drying conditions on the fruits microstructure

The cellulosic and pectic polymers of cellular structures which build plant tissues are prone to detrimental effects by a thermal process. Therefore, the drying causes many changes in the structure and properties of plant material [63]. The effects of drying on microstructure and distribution of cells in fresh and dried AOBs are shown in Fig. 1. As mentioned in (Fig. 1), the SEM micrographs on the surfaces of fresh and dried AOBs at four temperatures (50, 60, 70, and 80 °C), and three air velocities showed a distinct difference in the microstructure of fruits subjected to different treatments (Fig. 1). Before the drying process, the fresh AOBs tissue showed a spongelike organized structure consisting of small and clear spherical to oval cells and intercellular spaces. These results agree with Ghellam and Koca [10], who found that the AOBs tissue before any extraction process showed a porous spongelike, round, and fairly uniform structure. Furthermore, the cells of the fresh fruit had fewer holes and empty spaces structures than cell structures with the convective-dried fruits, which became very large; this finding was also reported by Deng and Zhao [64]. The hole depth increase when the drying temperature and air velocity increase. Our previous study [12] showed that the drying treatments of autumn olive berries caused important changes in their microstructure; the cells became very large, deformed, irregular, and wrinkling. Thus, the results show that the difference for fresh AOBs in terms of the structural characteristics is significantly different from convective-dried fruits material. Therefore, it can be concluded that the dried fruits under varying conditions caused severe shrinkage and fruit tissue anisotropic collapse.

Fig. 5 Drying curves of autumn olive fruits

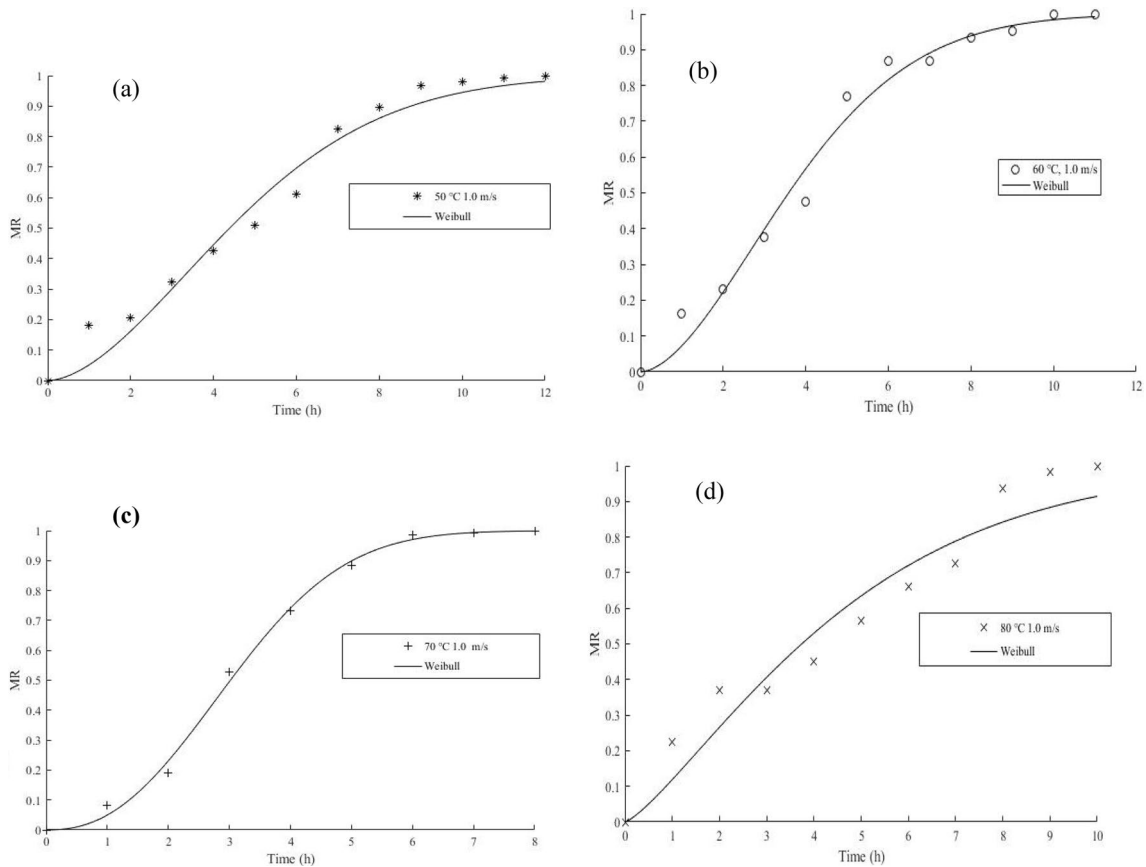
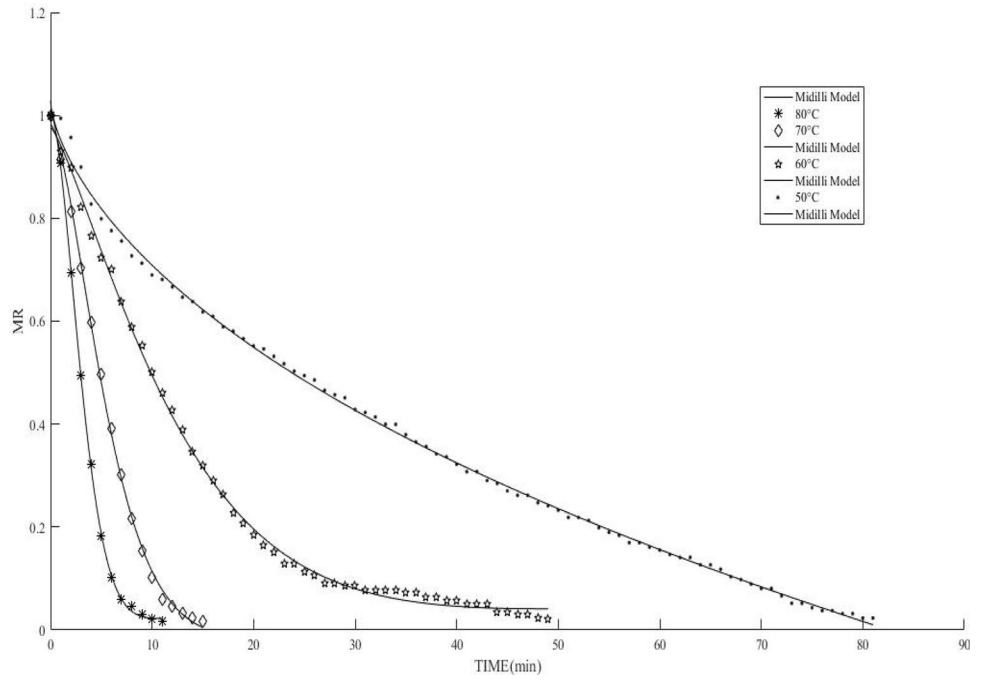


Fig. 6 Rehydration curves changes in moisture content of dried samples for different temperatures and the same air velocity of 1.0 m/s of 50 °C (a), 60 °C (b), 70 °C (c), and 80 °C (d)

Table 5 Mathematical models for rehydration kinetics

Model	Drying temperature (°C)	Air velocity, m/s	R ²	RMSE	X ²	Constants	
Peleg	50	0.5	0.967958	0.059851	0.003582	a=2.4809 b=0.77462	
		1.0	0.972361	0.062287	0.003879	a=3.7679 b=0.59565	
		1.5	0.987957	0.036910	0.001362	a=3.3094 b=0.70086	
	60	0.5	0.990785	0.032562	0.001060	a=4.9854 b=0.5875	
		1.0	0.966635	0.058860	0.003464	a=1.6522 b=0.86289	
		1.5	0.983289	0.041005	0.001681	a=4.1304 b=0.69763	
	70	0.5	0.991244	0.033327	0.001110	a=5.0425 b=0.57224	
		1.0	0.992275	0.029495	0.000869	a=1.6899 b=0.82144	
		1.5	0.988139	0.403827	0.163077	a=0.27038 b=-0.17292	
	80	0.5	0.982223	0.042060	0.001769	a=0.36351 b=-0.24164	
		1.0	0.986132	0.035523	0.001261	a=2.4584 b=0.80883	
		1.5	0.982223	0.042060	0.001769	a=3.0318 b=0.77145	
	Firstorderkinetic	50	0.5	0.976585	0.049156	0.002416	a=0.33369
			1.0	0.961355	0.070224	0.004931	a=0.2886
			1.5	0.988135	0.035075	0.001230	a=0.2801
60		0.5	0.978006	0.047964	0.002300	a=0.21536	
		1.0	0.970087	0.053359	0.002847	a=0.4177	
		1.5	0.974845	0.048168	0.002320	a=0.22126	
70		0.5	0.978779	0.049470	0.002447	a=0.21811	
		1.0	0.998235	0.013442	0.000180	a=0.44748	
		1.5	0.975084	0.023877	0.002124	a=0.963126	
80	0.5	0.998236	0.0134428	0.000180	a=0.44748		
	1.0	0.9788	0.049471	0.002447301	a=0.21811		
	1.5	0.97017	0.05331	0.002850	a=0.4177		
Exponential related equation	50	0.5	0.976585	0.049156	0.00241	a=0.33368	
		1.0	0.96135	0.070224	0.00493	a=0.28857	
		1.5	0.988135	0.035075	0.001230	a=0.28011	
	60	0.5	0.978006	0.047964	0.00230	a=0.21537	
		1.0	0.970087	0.053359	0.002847	a=0.41769	
		1.5	0.974845	0.048168	0.002320	a=0.22126	

Table 5 (continued)

Model	Drying temperature (°C)	Air velocity, m/s	R ²	RMSE	X ²	Constants	
Exponentialmodel	70	0.5	0.978779	0.049470	0.002447	a=0.2181	
		1.0	0.998235	0.013442	0.000180	a=0.44749	
		1.5	0.976317	0.047879	0.002292	a=0.25571	
	80	0.5	0.992533	0.026394	0.000697	a=0.27354	
		1.0	0.995738	0.018677	0.000349	a=0.31264	
		1.5	0.992533	0.026394	0.000697	a=0.27352	
	50	0.5	0.5	0.980628	0.046537	0.002165	a=0.27598 k=1.149
			1.0	0.996866	0.020971	0.000439	a=0.13672 k=1.5317
			1.5	0.992946	0.028248	0.000797	a=0.22457 k=1.1505
		60	0.5	0.981838	0.045714	0.002089	a=0.17116 k=1.1294
			1.0	0.970889	0.054979	0.003022	a=0.44684 k=0.93457
			1.5	0.975138	0.050017	0.002501	a=0.23442 k=0.96769
		70	0.5	0.988569	0.038079	0.001450	a=0.15552 k=1.2014
			1.0	0.998568	0.012697	0.000161	a=0.42725 k=1.0465
			1.5	0.997987	0.041846	0.002039	a=0.2031 k=1.1416
80	0.5	0.997142	0.016866	0.000284	a=0.21488 k=1.1594		
	1.0	0.996207	0.018128	0.000328	a=0.29034 k=1.0491		
	1.5	0.997142	0.016866	0.000284	a=0.2149 k=1.1593		
Weibull	50	0.5	0.980628	0.046537	0.002165	a=1.1491 b=3.0663	
		1.0	0.995444	0.0211911	0.0004490	a=1.1663 b=3.7878	
		1.5	0.994112	0.0243911	0.0005949	a=1.303 b=4.0809	
	60	0.5	0.981838	0.045714	0.002089	a=1.1295 b=4.7722	
		1.0	0.989987	0.030185	0.000911	a=0.93467 b=2.3677	

Table 5 (continued)

Model	Drying temperature (°C)	Air velocity, m/s	R ²	RMSE	X ²	Constants
Proposed model	70	1.5	0.99686	0.020972	0.000439	a = 1.5317 b = 3.6661
		0.5	0.991256	0.031387	0.000985	a = 1.0465 b = 2.2537
	80	1.0	0.998568	0.012697	0.000161	a = 1.0465 b = 2.2537
		1.5	0.997986	0.0135057	0.0001824	a = 1.1137 b = 2.2224
		0.5	0.997142	0.016866	0.000284	a = 1.0491 b = 3.2505
		1.0	0.996208	0.019274	0.000371	a = 1.0783 b = 3.259
		1.5	0.997142	0.016866	0.000284	a = 0.91599 b = 0.0011511
		50	0.5	0.9875095	0.0390304	0.0015233
	60	1.0	0.9935586	0.0316962	0.0010046	a = 1.1494 b = 7.7255 k = 1.6848
		1.5	0.9923784	0.0307967	0.0009484	a = 1.1849 b = 4.3944 k = 1.2723
		0.5	0.9888200	0.0378069	0.0014293	a = 1.8622 b = 3.8383 k = 0.707
		1.0	0.9830526	0.0439975	0.0019357	a = 1.0442 b = 5.1863 k = 1.8188
1.5		0.989473	0.033909	0.00115	a = 1.2334 b = 3.6822 k = 1.1018	
70		0.5	0.9927661	0.0319318	0.0010196	a = 1.4231 b = 4.5776 k = 0.98634
		1.0	0.9972124	0.0186780	0.0003488	a = 1.0625

Table 5 (continued)

Model	Drying temperature (°C)	Air velocity, m/s	R ²	RMSE	X ²	Constants
						b = 3.8111
						k = 1.7197
		1.5	0.9868890	0.4539043	0.2060291	a = 29126
						b = 11.5936
						k = 0.53851
	80	0.5	0.9794817	0.4529704	0.2051822	a = 6.3738
						b = 2.8033
						k = 0.50037
		1.0	0.9778945	0.5104193	0.2605279	a = 142.3302
						b = 7.2839
						k = 1.3783
		1.5	0.9499146	0.5921125	0.3505973	a = 0.0469
						b = 10.647
						k = 0.44864

Surface area and shrinkage of fruits

It has previously been observed that drying causes physical changes in the structure of plant material [65], including shrinkage [63]. The most important physical change in food during drying due to moisture evaporation from a food material is shrinkage [66]. The drying of autumn olive causes significant changes in the size of the cells and their distribution. In reviewing the literature published, specific correlations for sweet cherry fruit volume and surface area changes [67]. Stresses of heat and moisture transfer cause change and decreases in the food product shape and dimensions into a cellular structure [68]. The slow drying rate and homogeneous moisture distribution in the fruit dried at low temperatures reduce internal stresses. This finding contradicts the previous study [67], which has suggested that volume and area changes do not depend on dehydration operating variables. Therefore, AOBs tend to reduce their volume and the phenomenon under the convective dryer. The area of convectively dried AOBs at 80 °C and air velocity of 1.5 m/s was 0.0019, about 22% lower than the raw material in the conducted investigations. In contrast, the dried fruits obtained using the air velocity of 1.5 m/s were shown lower surface area values; this finding was also reported by Ratti [24]. The shrinkage of AOBs during convective drying is shown in (Table 7). The degree of shrinkage ranged between 59.52% at 50 °C and 1.0 m/s and 78.57 at 80 °C and 1.5 m/s on convective dried autumn olive (Table 7). In convective

drying at 80 °C and air velocity of 1.5 m/s, the cell walls showed high shrink due to high drying temperature. The air velocity of 1.5 m/s presented the highest shrinkage for all dried samples than other air velocities. The long drying time and high drying temperature may promote more water loss (Table 7). Thus, the increase in drying temperature leads to more shrinkage of convective dried samples at different drying conditions.

Total color change (ΔE), chromaticity (C), and hue angle

The color parameters of the dried autumn olive fruits under different experimental conditions are shown in Table 8. As seen in Table 8, Irrespective of drying conditions, the color parameters L*, a*, and b* were lower in dried autumn olive fruits than in fresh fruits, which means the fruits darkened. The L* and a* values increased, and b* values decreased when drying temperature and drying time decreased (Table 8). A decrease in the L* value indicates the darker color of the dried fruit. These results show that increasing drying time increases degradations due to longer exposure to temperature, which is consistent with Dadali et al. [69]. While fresh fruits had high color values, the color value decreased with the drying process in all dried samples. Chen et al. [70] reported that the L* value of dried jujube fruits increased after drying. The total color change

Table 6 Textural properties of autumn berries under different drying conditions

Temperature (°C)	Air velocity (m/s)	Hardness (N)	Springiness	Cohesiveness	Gumminess	Chewiness	Resilience
Fresh	–	206.39 ± 49.854g	0.813 ± .0115ab	0.673 ± 0.11abcd	138.11 ± 31.477def	112.48 ± 23.90cd	0.326 ± 0.0057a
50	0.5	371.51 ± 90.516gf	0.796 ± .0051ab	0.7760.041a	330.613 ± 136.66def	426.93 ± 244.48bc	0.253 ± 0.0057cba
	1.0	1019.01 ± 173.70gfe	0.87 ± 0.0614a	0.73 ± 0.214abcd	773.15 ± 256.14de	667.06 ± 186.82bc	0.303 ± 0.0085ba
	1.5	1234.58 ± 58.06efg	0.713 ± 0.0347abc	0.823 ± 0.289a	905.15 ± 54.84cde	645.37 ± 218.74 bc	0.18 ± 0.0016ed
60	0.5	1692.36 ± 88.66ef	0.586 ± .0126cd	0.58 ± 0.060abcd	969.8 ± 63.283ecd	573.82 ± 146.14bc	0.16 ± 0.03ed
	1.0	1813.69 ± 65.08e	0.666 ± 0.015bc	0.566 ± 0.032abcd	768.39 ± 85.609de	494.5 ± 27.5308bc	0.186 ± 0.02ed
	1.5	2373 ± 1.600e	0.64 ± 0.062bcd	0.573 ± 0.057abc	1169.88 ± 119.71cde	651.78 ± 25.330bc	0.153 ± 0.005ed
70	0.5	2213.27 ± 23.051de	0.603 ± .0722abc	0.432 ± .091defg	1178.03 ± 363.75cde	741.50 ± 224.86bc	0.174 ± 0.044ed
	1.0	2510.14 ± 43.237 de	0.566 ± 0.011c	0.416 ± 0.011dfg	1445.64 ± 285.02bcd	813.956 ± 149.4b c	0.166 ± 0.005e
	1.5	3786.57 ± 812.96cd	0.54 ± 0.0519cd	0.423 ± 0.064efg	2477.92 ± 747.65abc	1185.46 ± 737.00ab	0.156 ± 0.061ed
80	0.5	5463.06 ± 1257.63ab	0.52 ± .0725cd	0.392 ± .093efg	2314.52 ± 895.03abc	1246.30 ± 576.39ab	0.167 ± 0.048ed
	1.0	4468.62 ± 258.42bc	0.47 ± 0.104f	0.416 ± 0.08efg	1476.47 ± 801.815bcd	861.62 ± 388.65bc	0.14 ± 0.03e
	1.5	6764.23 ± 713.47a	0.57 ± 0.026cd	0.336 ± 0.125g	2989.163 ± 558.11a	1691.83 ± 330.80a	0.206 ± 0.0351edc

Data with the same superscript letters in a column are not significantly different ($p > 0.05$)

(ΔE) obtained during different drying conditions is presented in Table 8. The total color change (ΔE) between fresh and dried samples was statistically significant ($p < 0.05$). As shown in Table 8, the total color difference (ΔE) increased when the drying temperature decreased at 50 °C, and the highest average difference was 10.89 ± 1.16 at 50 °C. The ΔE average values of samples dried at 60 and 70 °C were 4.01 ± 1.33 and 4.72 ± 1.35 , respectively. Also, the ΔE value slightly increased with drying temperature at 80 °C to 7.52 ± 1.40 .

Antioxidant properties of dried *E. umbellata* fruits

According to Pei et al. [2] and Fordham et al. [16], *E. umbellata* contain high total phenols, polyphenols and is rich in α - and γ -tocopherols, as well as lycopene. However, whether other potential components such as bioactive compounds, changes, and properties are still unknown, this study provides an understanding of the properties (total phenol, total flavonoid, lycopene, and antioxidant capacity) of dried fruits at four different drying temperatures (50, 60, 70 and 80 °C) and three air velocities (0.5, 1.00 and 1.5 m/s). The flavonoid content ranged from 4370.69 mg/kg in the fresh sample to 1976.91 mg/kg in the dried samples (Table 9). The results showed that drying the sample at 60 °C and air velocity (1.5 and 0.5 m/s) guaranteed higher flavonoid content than other drying conditions. Antioxidant data of dried autumn olive samples are given in Table 9. Inhibition of DPPH and FRAP values showed relatively wide variation between samples. When DPPH is measured, the antioxidant activity yields 59.82 (mmol/g) of dried fruits at 80 °C and 1 m/s. This finding was supported by previous research on the drying of red pepper, in which Vega-Gálvez [71] found samples dried at 80 and 90 °C exhibit higher DPPH radical

scavenging activity. Moreover, FRAP at 80 °C and 1 m/s is measured, and the antioxidant activity of dried fruits is 44.60 mmol/g. Fruits dried at 80 °C, 1.5 air velocity have the highest lycopene content (518.52 mg/kg), followed by 470.29 fruits dried at 80 °C, 1.0 air velocity. This finding indicates that the antioxidant activity of dried AOBs is riched of antioxidants; this finding was similar and compatible with Gamba et al. [9]. Results showed that drying fruits at 80 °C temperature had significant antioxidant compounds and antioxidant capacity of DPPH and FRAP values than in other drying conditions. Table 9 shows that according to the effect of drying temperature, there is a statistical difference between the averages of total phenolic, total flavonoid, FRAP, DPPH, and lycopene contents, respectively. The hot air drying method can affect the antioxidant quality of samples depending on the temperature applied and the type of sample [72–74]. Our results proved that the increase in drying temperature was positively correlated with the antioxidant properties. The increase in the drying temperature led to a reduction in the drying time, thus less exposure of AOBs fruits to the heat, guaranteeing the preservation of antioxidants. Moreover, the reduction of water content reduces the microbial degradation of antioxidants and limits enzymatic activity [12]. Our findings are found in the same agreement with Vu et al. [75], who suggest that the dried banana peels at higher drying temperature within a short time could retain higher TPC, TFC, and proanthocyanidin levels.

Effects of drying on phenolic compounds

Previous studies evaluated the *E. umbellata* as a rich source of phenolic compounds [9, 15]. The autumn olive berries contain major phenolic compounds monomers

such as proanthocyanidins and (+)-catechin and (–)-epicatechin [2]. Antioxidant activity of jujube fruits, similarly to content, was related to the drying methods [70]. According to Valadez-Carmona et al. [76], the food processing techniques might cause positive, neutral, and negative effects on the retention of phenolic compounds in vegetables and fruits. The effect of different drying temperatures on phenolic compounds is shown in Table 10, identified as gallic acid, catechin, vanillic acid, p-coumaric acid, benzoic acid, salicylic acid, ellagic acid, quercetin-3glukoside and resveratrol, respectively. The present study found that the phenolic compounds among drying conditions showed significant differences between the fresh samples and evaluated drying temperatures. Ishaq et al. [47] reported that gallic acid is the major antioxidant component in autumn olive fruits. As seen in Table 10, all the phenolic compounds of *E. umbellata* fruits are affected by drying conditions due to decreasing values except for catechin and increased p-coumaric acid. Hot air drying may also decrease the phenolic compounds [77], attributed to both oxidation and release of free phenolic compounds [78]. The fresh AOBs showed the highest values of phenolic compounds such as gallic acid, vanillic acid, benzoic acid, salicylic acid, and ellagic acid, quercetin3glukoside, and resveratrol were 4.59, 5.72, 13.62, 4.98, 46.80, 9.46 and 6.86 mg/kg, respectively. On the other hand, Catechin and p-coumaric acid values were higher in dried AOBs than in fresh fruits (Table 10). The samples dried at 80 °C and air velocity 1.0 m/s had high gallic acid, catechin, benzoic acid, salicylic acid, ellagic acid, and quercetin-3glukoside 6.57, 9.66, 1.80, 2.13, 37.24, and 8.83 mg/kg, respectively. The AOBs dried at 70 °C and air velocity 1.0 m/s showed 8.99, 4.83 mg/kg p-coumaric acid, and resveratrol, respectively. Garau et al. [79] reported that the longer exposure to heat when drying at low temperatures might stimulate the degradation of phytochemicals. According to the results mentioned above, the AOBs dried at 80 °C showed higher values of phenolic compounds.

Conclusion

This paper assessed the physical, textural, morphological, and bioactive properties and optimum conditions of convective drying and rehydration of AOBs. The results found

Table 7 Shrinkage of AOBs under different drying conditions

Temperature (°C)	Air velocity (m/s)	Shrinkage, (%)
50	0.5	61.91 ± 4.12cd
	1.0	59.52 ± 8.25de
	1.5	69.05 ± 4.12bcd
60	0.5	59.52 ± 4.12de
	1.0	61.90 ± 4.12cd
	1.5	71.43 ± 0.00abcd
70	0.5	69.05 ± 4.12bcd
	1.0	71.43 ± 0.00abcd
	1.5	73.81 ± 4.12abc
80	0.5	76.19 ± 4.12ab
	1.0	76.19 ± 4.12ab
	1.5	78.57 ± 0.00ab

According to the effect of temperature, there is no statistical difference between the averages shown with the same letter in the same column ($p > 0.05$)

that the drying conditions significantly affect the retention of texture, microstructure, total phenolic, total flavonoid, lycopene content, gallic acid, catechin, benzoic acid, salicylic acid, Ellagic acid, and quercetin3-glucoside, and antioxidant properties (measured by FRAP, and DPPH) of autumn olive fruits. The study discovered that the optimum drying conditions for AOBs with the highest antioxidant properties were 80 °C and 1.5 m/s. As a result, convective drying at 80 °C and 1.5 m/s is recommended for drying AOBs. Furthermore, the change in air velocity was not observed to significantly influence the fruit s microstructure, total color change, shrinkage, or antioxidant properties among the different dried samples. The present study has found that generally, the moisture content of *E. umbellata* decreased continuously with drying time. Midilli and Weibull models were the most fitted models to describe the drying and rehydration behaviors of AOBs, respectively. The evidence from this study suggests a significant opportunity to advance understanding of the drying characteristic of the convective dried autumn olive fruit and contribute to the literature. Further research could also be conducted to determine the effectiveness of different drying methods for autumn olive fruits. Overall, convective drying can be applied at 80 °C for industrial drying of *E. umbellata* fruits as a good source of various nutrients and antioxidant compounds.

Table 8 The effect of different drying conditions on the color of AOBs

	L*	a*	b*	ΔE	Chroma	Hue
50						
0.5	33.81 ± 1.19b	5.25 ± 0.52c	10.04 ± 0.81a	11.79 ± 0.94a	11.35 ± 0.51ed	62.28 ± 4.15a
1	35.99 ± 0.65b	5.97 ± 0.77c	9.64 ± 0.88ab	9.79 ± 0.90b	11.36 ± 0.76ed	58.19 ± 4.47b
1.5	34.62 ± 1.09b	5.56 ± 1.01c	9.33 ± 0.28ab	11.09 ± 0.74ab	10.89 ± 0.42e	59.31 ± 5.01b
60						
0.5	40.61 ± 1.43a	9.51 ± 0.84b	8.51 ± 1.10abc	5.02 ± 0.74e	12.76 ± 1.3dc	41.74 ± 2.04c
1	40.08 ± 0.24a	11.79 ± 0.82 ab	9.45 ± 0.50abc	3.23 ± 0.71f	15.11 ± 0.89a	38.75 ± 1.37c
1.5	40.58 ± 1.74a	11.57 ± 2.76 ab	9.41 ± 1.12abc	3.79 ± 1.87fe	14.93 ± 2.84ab	39.54 ± 3.35c
70						
0.5	39.61 ± 2.34a	11.81 ± 0.63 ab	8.38 ± 0.65dc	4.39 ± 1.80ef	14.50 ± 0.17ab	35.38 ± 3.54d
1	38.53 ± 2.58a	11.84 ± 1.48 ab	8.51 ± 0.34cb	5.25 ± 1.83e	14.60 ± 1.02ab	35.91 ± 4.45d
1.5	40.96 ± 1.54a	11.61 ± 1.23ab	7.49 ± 0.88d	4.51 ± 0.29e	13.86 ± 0.68cba	32.95 ± 5.59e
80						
0.5	40.37 ± 1.78a	13.02 ± 1.53a	5.42 ± 1.15e	6.36 ± 0.77d	14.14 ± 1.43cba	22.73 ± 5.27f
1	41.94 ± 2.61a	12.12 ± 1.83ab	3.93 ± 0.73f	7.61 ± 1.37cd	12.75 ± 1.97ab	17.91 ± 0.67g
1.5	40.09 ± 3.04a	10.71 ± 0.56ab	3.53 ± 0.61f	8.58 ± 1.27c	11.29 ± 0.38edc	18.30 ± 3.74g

There is no statistical difference between the averages of drying conditions indicated with the same letter in the same column (p > 0.05)

Table 9 Antioxidant properties of dried AOBs in different conditions

Temperature (°C)	Air velocity (m/s)	Total phenolic, mg/kg	Total flavonoid, mg/kg	FRAP, mmol/g	DPPH, mmol/g	Lycopene, mg/kg
50	0.5	59546.67 ± 925.42g	1719.63 ± 212.80	26.47 ± 2.02d	44.95 ± 2.70bc	365.42 ± 58.22bcd
	1.0	62883.33 ± 3620.73fg	1823.45 ± 314.75	30.25 ± 1.52cd	44.12 ± 1.25c	349.40 ± 65.67bcd
	1.5	60316.66 ± 1176.19g	1561.66 ± 238.53	37.52 ± 2.27abc	44.02 ± 0.31c	397.49 ± 81.46abcd
60	0.5	68444.45 ± 7632.69gfe	1958.85 ± 113.56	38.88 ± 3.35ab	43.19 ± 3.70c	331.09 ± 26.68bcd
	1.0	66391.11 ± 5695.07gfe	1683.53 ± 127.98	40.67 ± 3.35ab	43.40 ± 3.87c	306.72 ± 82.06dc
	1.5	77513.33 ± 5558.48edc	1976.91 ± 348.12	40.91 ± 0.44ab	49.91 ± 1.93abc	391.37 ± 55.05abcd
70	0.5	81620.00 ± 1429.06dc	1706.10 ± 162.48	38.59 ± 1.98ab	52.80 ± 0.47abc	283.99 ± 38.80d
	1.0	74690.00 ± 2475.20fed	1710.61 ± 109.45	39.66 ± 2.07bc	50.63 ± 4.94abc	325.41 ± 24.29bcd
	1.5	84528.89 ± 4235.65dc	1638.39 ± 169.66	34.86 ± 3.51bc	55.17 ± 4.62ab	359.58 ± 33.53bcd
80	0.5	101982.20 ± 4425.79a	1728.66 ± 265.79	38.68 ± 2.90ab	59.20 ± 3.41a	442.11 ± 26.92abc
	1.0	88122.22 ± 901.38bc	1719.64 ± 115.69	37.52 ± 0.67abc	59.82 ± 1.55a	470.29 ± 26.00ab
	1.5	99672.22 ± 3596.39ab	1651.94 ± 217.91	44.60 ± 4.54a	55.17 ± 7.78ab	518.52 ± 37.46a

According to the effect of drying conditions, data with the same lowercase letters in a column are not significantly different (p > 0.05)

Table 10 Effect of drying conditions on AOBs phenolic compounds

Temperature (°C)	Air velocity, m/s	Galic acid	Catechin	Vanillic acid	p-coumaric acid	Benzoic acid	Salisilic acid	Ellagic acid	Quercetin:3glucoside	resveratrol
Fresh sample	0	4.59 ± 0.15c	0.43 ± 0.04h	5.72 ± 0.30a	2.67 ± 0.18e	13.62 ± 0.88a	4.98 ± 0.38a	46.80 ± 0.52a	9.46 ± 0.23a	6.86 ± 0.40a
50	0.5	5.01 ± 0.05b	8.27 ± 0.25abc	0.64 ± 0.04bc	6.72 ± 0.11bc	1.61 ± 0.11bc	1.88 ± 0.28bc	27.24 ± 0.62bcd	2.93 ± 0.71bcd	1.87 ± 0.35c
	1.0	2.98 ± 0.18d	4.91 ± 0.02cde	0.40 ± 0.02c	8.17 ± 0.19ab	0.55 ± 0.14e	0.96 ± 0.05de	26.94 ± 0.46bcd	2.71 ± 0.71bcd	1.94 ± 0.57c
	1.5	2.02 ± 0.04e	8.98 ± 1.33ab	0.26 ± 0.01c	6.38 ± 0.59bcd	0.75 ± 0.01f	0.93 ± 0.05de	27.55 ± 0.54bcd	2.71 ± 0.71bcd	1.66 ± 0.14c
60	0.5	2.04 ± 0.0e	3.96 ± 0.26g	0.90 ± 0.06b	3.09 ± 0.05e	0.89 ± 0.01def	0.62 ± 0.13e	12.46 ± 0.31g	1.88 ± 0.08cde	2.11 ± 0.82c
	1.0	1.61 ± 0.5cde	6.63 ± 0.41bc	0.37 ± 0.05	2.68 ± 0.11e	1.08 ± 0.13cdef	0.92 ± 0.02de	25.04 ± 0.69cde	2.14 ± 0.14bcde	2.18 ± 1.10c
	1.5	0.40 ± 0.00f	4.62 ± 0.31gf	0.52 ± 0.02bc	6.26 ± 0.22bcd	1.03 ± 0.15cdef	0.71 ± 0.02e	25.17 ± 0.68cde	2.15 ± 0.23bcde	2.83 ± 0.53c
70	0.5	1.79 ± 0.13e	7.48 ± 0.19bcd	0.27 ± 0.02c	3.41 ± 0.11e	0.90 ± 0.03cdef	0.97 ± 0.11de	20.41 ± 0.16def	1.55 ± 1.12cde	2.03 ± 0.22c
	1.0	1.93 ± 0.09e	5.03 ± 0.73cd	0.39 ± 0.02c	8.99 ± 0.02a	1.47 ± 0.01bcde	0.79 ± 0.10de	19.17 ± 0.86def	1.87 ± 0.62de	4.83 ± 0.57b
	1.5	1.41 ± 0.05e	7.28 ± 0.06gf	0.5 ± 0.06bc	2.88 ± 0.10e	0.99 ± 0.01cdef	1.08 ± 0.21bc	18.31 ± 0.95def	1.87 ± 0.83de	1.63 ± 0.56c
80	0.5	5.26 ± 0.02d	4.73 ± 0.55bcd	0.49 ± 0.03bc	6.05 ± 0.08d	1.77 ± 0.03bcd	1.13 ± 0.03bc	17.87 ± 0.75fg	8.14 ± 0.42ab	1.83 ± 0.69c
	1.0	6.57 ± 0.51a	9.66 ± 0.41a	0.48 ± 0.01c	6.50 ± 0.69bcd	1.80 ± 0.28b	2.13 ± 0.08b	37.24 ± 1.61ab	8.83 ± 0.92ab	2.02 ± 1.11c
	1.5	4.57 ± 0.01cb	6.02 ± 0.97cdef	0.34 ± 0.01c	3.31 ± 0.07e	0.71 ± 0.18ef	1.65 ± 0.02bc	29.80 ± 0.51bc	7.99 ± 0.17ab	1.96 ± 0.52c

Retention times (RT, min) 4.63, 14.67, 23.40, 32.95, 16.86, 44.06, 34.02, 28.41, and 55.47 correspond to gallic acid, catechin, vanillic acid, p-coumaric acid, benzoic acid, salisilic acid, ellagic acid, quercetin:3glucoside, and resveratrol, respectively

Different lowercase letters in the same column mean statistical difference at $p \leq 0.05$

Funding This research was funded by [Ondokuz Mayıs University project office] grant number [PYO. MUH.1904.20.007].

References

- M.R. Moore et al., Distribution and growth of autumn olive in a managed forest landscape. *For. Ecol. Manage.* **310**, 589–599 (2013)
- R. Pei et al., Phenolic and tocopherol content of autumn olive (*Elaeagnus umbellata*) berries. *J. Funct. Foods* **16**, 305–314 (2015)
- Fordham, I.M., et al. *Autumn olive: a potential alternative crop*. in *XXVI International Horticultural Congress: Berry Crop Breeding, Production and Utilization for a New Century* 626. 2002.
- V.R. de Souza et al., Determination of the bioactive compounds, antioxidant activity and chemical composition of Brazilian blackberry, red raspberry, strawberry, blueberry and sweet cherry fruits. *Food Chem.* **156**, 362–368 (2014)
- S.D. Ahmad et al., Morphological and biochemical variations in *Elaeagnus umbellata* Thunb. from mountains of Pakistan. *Acta Bot. Croat.* **64**(1), 121–128 (2005)
- D. Donno et al., *Currants and strawberries as bioactive compound sources: Determination of antioxidant profiles with HPLC-DAD/MS*. *J. Appl. Bot. Food Qual.* **86**, 1–10 (2013). <https://doi.org/10.5073/jabfq.2259.86.1>
- C. Liu et al., *Artemisia judaica* L.: micropropagation and antioxidant activity. *J. Biotechnol.* **110**(1), 63–71 (2004)
- M.L. Nguyen, S.J. Schwartz, Lycopene: chemical chemical and biological properties: developing nutraceuticals for the new millennium. *Food Technol. (Chicago)* **53**(2), 38–45 (1999)
- G. Gamba et al., Phytochemical characterization and bioactivity evaluation of autumn olive (*Elaeagnus umbellata* Thunb.) *Pseudodrupes* as potential sources of health-promoting compounds. *Appl. Sci.* (2020). <https://doi.org/10.3390/app10124354>
- M. Ghellam, İ Koca, Autumn olive berries: characterization, antioxidant capacity, optimization of solvents and extraction conditions of lycopene. *J. Food Measure. Characteriz.* **16**, 1–11 (2021)
- S. Ahmad, S. Sabir, M. Zubair, Ecotypes diversity in autumn olive (*Elaeagnus umbellata* Thunb.): a single plant with multiple micro-nutrient genes. *Chem. Ecol.* **22**(6), 509–521 (2006)
- O. Zannou et al., Optimization of drying temperature for the assessment of functional and physical characteristics of autumn olive berries. *J. Food Process. Preserv.* **45**(9), e15658 (2021)
- S.M. Sabir, S.D. Ahmad, 16 functional foods based on sea buckthorn (*Hippophae rhamnoides* ssp. turkestanica) and Autumn Olive (*Elaeagnus umbellata*). *Funct. Foods East* (2010). <https://doi.org/10.1201/b10264-17>
- N. Nazir et al., Curative effect of catechin isolated from *Elaeagnus umbellata* Thunb. berries for diabetes and related complications in streptozotocin-induced diabetic rats model. *Molecules* **26**(1), 137 (2020)
- V. Spinola et al., Changes in the phenolic compositions of *Elaeagnus umbellata* and *Sambucus lanceolata* after in vitro gastrointestinal digestion and evaluation of their potential anti-diabetic properties. *Food Res. Int.* **122**, 283–294 (2019)
- I.M. Fordham et al., Fruit of autumn olive: a rich source of lycopene. *HortScience* **36**(6), 1136–1137 (2001)
- Dauthy, E., *FAO Agricultural Services Bulletin No. 119*. Food and Agriculture Organization of the United Nations, 1995.
- M. Hatamipour et al., Drying characteristics of six varieties of sweet potatoes in different dryers. *Food Bioprod. Process.* **85**(3), 171–177 (2007)
- Ndukwu, M.C., *Effect of drying temperature and drying air velocity on the drying rate and drying constant of cocoa bean*. *Agricultural Engineering International: CIGR Journal*, XI, Manuscript 1091 (2009)
- D. Jayas, S. Sokhansanj, Thin-layer drying of barley at low temperatures. *Can. Agric. Eng.* **31**(1), 21–23 (1989)
- R.N. Putra, T.A. Ajiwiguna, Influence of air temperature and velocity for drying process. *Procedia Eng.* **170**, 516–519 (2017)
- M. Khraishesh, T. Cooper, T. Magee, Shrinkage characteristics of potatoes dehydrated under combined microwave and convective air conditions. *Drying Technol.* **15**(3–4), 1003–1022 (1997)
- A. Castro, E. Mayorga, F. Moreno, Mathematical modelling of convective drying of feijoa (*Acca sellowiana* Berg) slices. *J. Food Eng.* **252**, 44–52 (2019)
- C. Ratti, Shrinkage during drying of foodstuffs. *J. Food Eng.* **23**(1), 91–105 (1994)
- H. Majdi, J.A. Esfahani, M. Mohebbi, Optimization of convective drying by response surface methodology. *Comput. Electron. Agric.* **156**, 574–584 (2019)
- B. Sturm, W.C. Hofacker, O. Hensel, Optimizing the drying parameters for hot-air-dried apples. *Drying Technol.* **30**(14), 1570–1582 (2012)
- K. Sacilik, A.K. Elicin, G. Unal, Drying kinetics of Üryani plum in a convective hot-air dryer. *J. Food Eng.* **76**(3), 362–368 (2006)
- H. Pashazadeh, O. Zannou, I. Koca, Modeling of drying and rehydration kinetics of *Rosa pimpinellifolia* fruits: toward formulation and optimization of a new tea with high antioxidant properties. *J. Food Process Eng.* **43**(10), e13486 (2020)
- Y. Wang et al., Effects of hot air and microwave-assisted drying on drying kinetics, physicochemical properties, and energy consumption of chrysanthemum. *Chem. Eng. Process Process Intensif.* **129**, 84–94 (2018)
- İ Doymaz, Convective drying kinetics of strawberry. *Chem. Eng. Process.* **47**(5), 914–919 (2008)
- S. Sahin, S.G. Sumnu, *Physical properties of foods* (Springer, Cham, 2006)
- L. Rolle et al., Instrumental texture analysis parameters as markers of table-grape and winegrape quality: a review. *Am. J. Enol. Vitic.* **63**(1), 11–28 (2012)
- A. Figiel, Dehydration of apples by a combination of convective and vacuum-microwave drying. *Polish J. Food Nutr. Sci.* **57**(4), 131–135 (2007)
- L. Meda, C. Ratti, Rehydration of freeze-dried strawberries at varying temperatures. *J. Food Process Eng.* **28**(3), 233–246 (2005)
- E. Lopez-Quiroga et al., Model discrimination for drying and rehydration kinetics of freeze-dried tomatoes. *J. Food Process Eng.* (2019). <https://doi.org/10.1111/jfpe.13192>
- A. Official, *Methods of analysis of AOAC International* (AOAC INTERNATIONAL, Maryland, 2003)
- H. Pashazadeh, O. Zannou, I. Koca, Modeling and optimization of drying conditions of dog rose for preparation of a functional tea. *J. Food Process Eng.* **44**(3), e13632 (2021)
- M. Ghellam, I. Koca, Modelling of rehydration kinetics of desert truffles (*Terfezia* spp.) dried by microwave oven. *Turkish J. Agric. Food Sci. Technol.* (2020). <https://doi.org/10.24925/turjaf.v8i2.407-415.3083>
- A.J. Rosenthal, Texture profile analysis—how important are the parameters? *J. Texture Stud.* **41**(5), 672–684 (2010)
- O. Zannou, I. Koca, Optimization and stabilization of the antioxidant properties from Alkanet (*Alkanna tinctoria*) with natural deep eutectic solvents. *Arab. J. Chem.* **13**(8), 6437–6450 (2020)
- O.A. Fawole, S.C. Riva, U.L. Opara, Efficacy of edible coatings in alleviating shrivel and maintaining quality of Japanese plum

- (*Prunus salicina* Lindl.) during export and shelf life conditions. *Agronomy* **10**(7), 1023 (2020)
42. S. Tural, I. Koca, Physico-chemical and antioxidant properties of cornelian cherry fruits (*Cornus mas* L.) grown in Turkey. *Sci. Horticult.* **116**(4), 362–366 (2008)
 43. X. Gao et al., Changes in antioxidant effects and their relationship to phytonutrients in fruits of sea buckthorn (*Hippophae rhamnoides* L.) during maturation. *J. Agric. Food Chem.* **48**(5), 1485–1490 (2000)
 44. M.-C. Wu et al., Proteomic analysis of up-accumulated proteins associated with fruit quality during autumn olive (*Elaeagnus umbellata*) fruit ripening. *J. Agric. Food Chem.* **59**(2), 577–583 (2011)
 45. S.Y. Wang, I.M. Fordham, Differences in chemical composition and antioxidant capacity among different genotypes of autumn olive (*Elaeagnus umbellata* Thunb.). *Food Technol. Biotechnol.* **45**(4), 402–409 (2007)
 46. K.F. Khattak, Free radical scavenging activity, phytochemical composition and nutrient analysis of *Elaeagnus umbellata* berry. *J. Med. Plants Res.* **6**(39), 5196–5203 (2012)
 47. S. Ishaq et al., Antioxidant properties of *Elaeagnus umbellata* berry solvent extracts against lipid peroxidation in mice brain and liver tissues. *Food Sci. Biotechnol.* **24**(2), 673–679 (2015)
 48. M.K. Gupta, V. Sehgal, S. Arora, Optimization of drying process parameters for cauliflower drying. *J. Food Sci. Technol.* **50**(1), 62–69 (2013)
 49. E. Horuz, M. Maskan, Hot air and microwave drying of pomegranate (*Punica granatum* L.) arils. *J. Food Sci. Technol.* **52**(1), 285–293 (2015)
 50. N. Izli et al., Effect of different drying methods on drying characteristics, colour, total phenolic content and antioxidant capacity of Goldenberry (*Physalis peruviana* L.). *Int. J. Food Sci. Technol.* **49**(1), 9–17 (2014)
 51. H. Pashazadeh, O. Zannou, I. Koca, Modeling of drying and rehydration kinetics of *Rosa pimpinellifolia* fruits: toward formulation and optimization of a new tea with high antioxidant properties. *J. Food Process Eng.* (2020). <https://doi.org/10.1111/jfpe.13486>
 52. İ Doymaz, Evaluation of some thin-layer drying models of persimmon slices (*Diospyros kaki* L.). *Energy Conv. Manage.* **56**, 199–205 (2012)
 53. F. Nurafifah, A.L. Chuah, M.P.F. Wahida, Drying of *Plectranthus amboinicus* (lour) spreng leaves by using oven dryer. *Eng. Agric. Environ. Food* **11**(4), 239–244 (2018)
 54. F. Chenlo et al., Air-drying and rehydration characteristics of the brown seaweeds, *Ascophyllum nodosum* and *Undaria pinnatifida*. *J. Appl. Phycol.* **30**(2), 1259–1270 (2018)
 55. P. García-Pascual et al., Morchella esculenta (morel) rehydration process modelling. *J. Food Eng.* **72**(4), 346–353 (2006)
 56. Y.-Y. Zhao et al., Improving of texture and rehydration properties by ultrasound pretreatment for infrared-dried shiitake mushroom slices. *Drying Technol.* **37**(3), 352–362 (2019)
 57. A. Benseddik et al., Empirical and diffusion models of rehydration process of differently dried pumpkin slices. *J. Saudi Soc. Agric. Sci.* **18**(4), 401–410 (2019)
 58. E. Lopez-Quiroga et al., Model discrimination for drying and rehydration kinetics of freeze-dried tomatoes. *J. Food Process Eng.* **43**(5), e13192 (2020)
 59. C. Contreras et al., Effect of vacuum impregnation and microwave application on structural changes which occurred during air-drying of apple. *LWT Food Sci. Technol.* **38**(5), 471–477 (2005)
 60. A. Gabas et al., Influence of drying conditions on the rheological properties of prunes. *Drying Technol.* **20**(7), 1485–1502 (2002)
 61. M. Zielinska, M. Markowski, D. Zielinska, The effect of freezing on the hot air and microwave vacuum drying kinetics and texture of whole cranberries. *Drying Technol.* **37**(13), 1714–1730 (2019)
 62. A.C. Cruz, R.P. Guiné, J.C. Gonçalves, Drying kinetics and product quality for convective drying of apples (cvs. Golden Delicious and Granny Smith). *Int. J. Fruit Sci.* **15**(1), 54–78 (2015)
 63. D. Witrowa-Rajchert, M. Rzaça, Effect of drying method on the microstructure and physical properties of dried apples. *Drying Technol.* **27**(7–8), 903–909 (2009)
 64. Y. Deng, Y. Zhao, Effect of pulsed vacuum and ultrasound osmopretreatments on glass transition temperature, texture, microstructure and calcium penetration of dried apples (Fuji). *LWT Food Sci. Technol.* **41**(9), 1575–1585 (2008)
 65. P.P. Lewicki, G. Pawlak, Effect of drying on microstructure of plant tissue. *Drying Technol.* **21**(4), 657–683 (2003)
 66. C.A. Márquez, A. De Michelis, Comparison of drying kinetics for small fruits with and without particle shrinkage considerations. *Food Bioprocess Technol.* **4**(7), 1212–1218 (2011)
 67. M. Ochoa et al., Analysis of shrinkage phenomenon of whole sweet cherry fruits (*Prunus avium*) during convective dehydration with very simple models. *J. Food Eng.* **79**(2), 657–661 (2007)
 68. T. Tsuruta, H. Tanigawa, H. Sashi, Study on shrinkage deformation of food in microwave–vacuum drying. *Drying Technol.* **33**(15–16), 1830–1836 (2015)
 69. G. Dadali, E. Demirhan, B. Özbek, Color change kinetics of spinach undergoing microwave drying. *Drying Technol.* **25**(10), 1713–1723 (2007)
 70. Q. Chen et al., Drying kinetics and quality attributes of jujube (*Zizyphus jujuba* Miller) slices dried by hot-air and short- and medium-wave infrared radiation. *LWT Food Sci. Technol.* **64**(2), 759–766 (2015)
 71. A. Vega-Gálvez et al., Mathematical modelling of mass transfer during rehydration process of Aloe vera (*Aloe barbadensis* Miller). *Food Bioprod. Process.* **87**(4), 254–260 (2009)
 72. C.I. Nindo et al., Evaluation of drying technologies for retention of physical quality and antioxidants in asparagus (*Asparagus officinalis*, L.). *LWT Food Sci. Technol.* **36**(5), 507–516 (2003)
 73. E. Capecka, A. Mareczek, M. Leja, Antioxidant activity of fresh and dry herbs of some *Lamiaceae* species. *Food Chem.* **93**(2), 223–226 (2005)
 74. S.P. Ong, C.L. Law, C.L. Hii, Optimization of heat pump–assisted intermittent drying. *Drying Technol.* **30**(15), 1676–1687 (2012)
 75. H.T. Vu, C.J. Scarlett, Q.V. Vuong, Effects of drying conditions on physicochemical and antioxidant properties of banana (*Musa cavendish*) peels. *Drying Technol.* **35**(9), 1141–1151 (2017)
 76. L. Valadez-Carmona et al., Effects of microwaves, hot air and freeze-drying on the phenolic compounds, antioxidant capacity, enzyme activity and microstructure of cacao pod husks (*Theobroma cacao* L.). *Innov. Food Sci. Emerg. Technol.* **41**, 378–386 (2017)
 77. D.K. Asami et al., Comparison of the total phenolic and ascorbic acid content of freeze-dried and air-dried marionberry, strawberry, and corn grown using conventional, organic, and sustainable agricultural practices. *J. Agric. Food Chem.* **51**(5), 1237–1241 (2003)
 78. C. Sun et al., Effect of ethanol/water solvents on phenolic profiles and antioxidant properties of Beijing propolis extracts. *Evid. Based Complement. Alternat. Med.* (2015). <https://doi.org/10.1155/2015/595393>
 79. M.C. Garau et al., Effect of air-drying temperature on physicochemical properties of dietary fibre and antioxidant capacity of orange (*Citrus aurantium* v. *Canoneta*) by-products. *Food Chem.* **104**(3), 1014–1024 (2007)
 80. T. Tunde-Akintunde, Mathematical modeling of sun and solar drying of chilli pepper. *Renew. Energy* **36**(8), 2139–2145 (2011)
 81. Y.G. Keneni, A.T. Hvoslef-Eide, J.M. Marchetti, Mathematical modelling of the drying kinetics of *Jatropha curcas* L. seeds. *Ind. Crops Prod.* **132**, 12–20 (2019)

82. Ld.N.S. Dorneles et al., Effect of air temperature and velocity on drying kinetics and essential oil composition of *Piper umbellatum* L. leaves. *Ind. Crops Prod.* **142**, 111846 (2019)
83. B.H. Samani et al., Development and optimization of the new ultrasonic-infrared-vacuum dryer in drying *Kelussia odoratissima* and its comparison with conventional methods. *Ind. Crops Prod.* **123**, 46–54 (2018)
84. M. Noshad et al., Kinetic modeling of rehydration in air-dried quinces pretreated with osmotic dehydration and ultrasonic. *J. Food Process. Preserv.* **36**(5), 383–392 (2012)
85. I.S. Saguy, A. Marabi, R. Wallach, New approach to model rehydration of dry food particulates utilizing principles of liquid

transport in porous media. *Trends Food Sci. Technol.* **16**(11), 495–506 (2005)

Publisher's Note Springer Nature remains neutral with regard to jurisdictional claims in published maps and institutional affiliations.

Springer Nature or its licensor holds exclusive rights to this article under a publishing agreement with the author(s) or other rightsholder(s); author self-archiving of the accepted manuscript version of this article is solely governed by the terms of such publishing agreement and applicable law.